

**Figure 9.** Variability indices defined in Sec. 2 as functions of magnitude for the TF1 dataset described in Sec. 3.1. Variable objects are marked with 'x'. The curves represent the expected value of an index as a function of magnitude and the selection threshold corresponding to the best trade-off between the completeness and purity of the candidates list ( $F_{\text{max}}$ , see Sec. 4, Fig. 10).

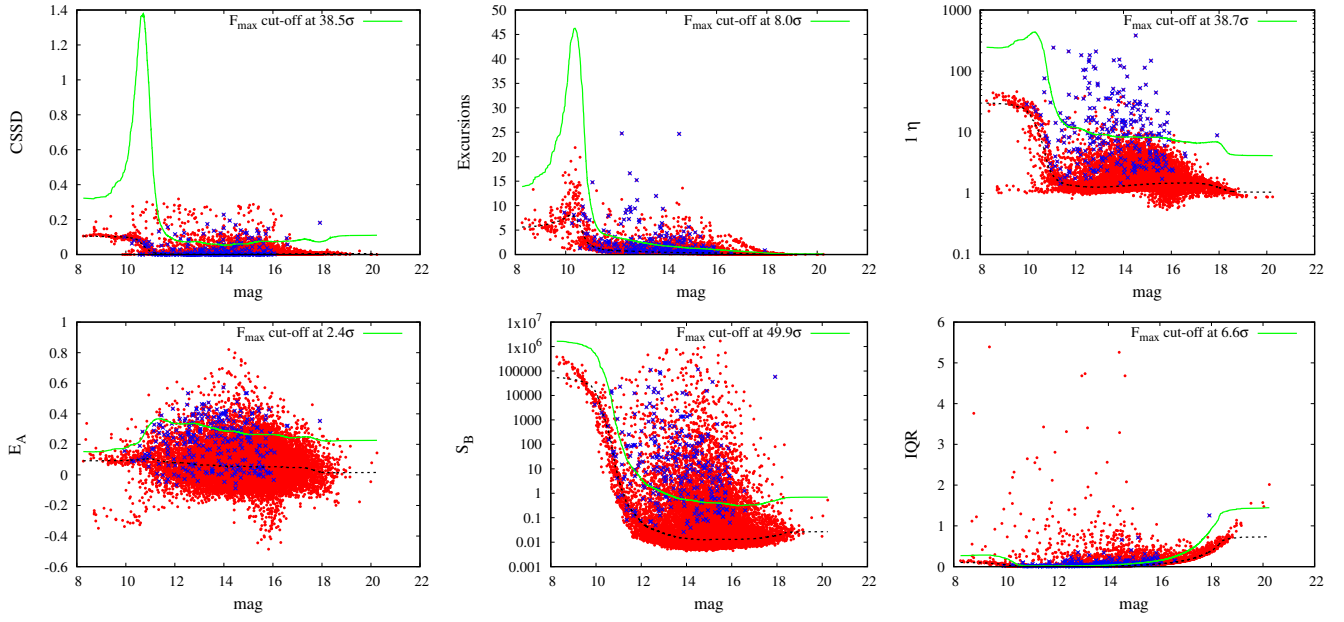
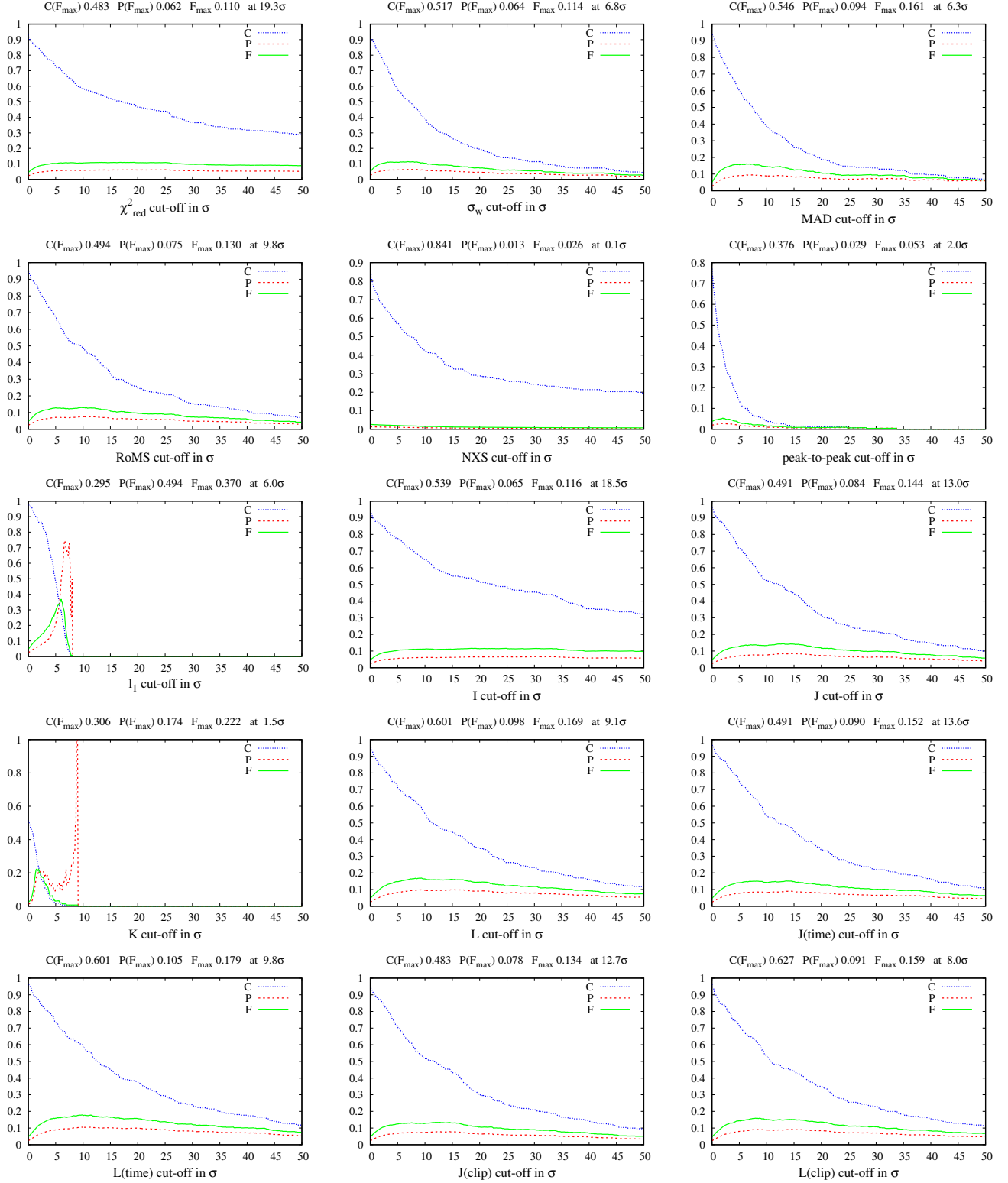


Figure 9. continued.





**Figure 10.** Variable star selection completeness (C), purity (P), and  $F_1$ -score (F, see Sec 4) as a function of selection threshold for the variability indices defined in Sec. 2 (TF1 dataset, Sec. 3.1).

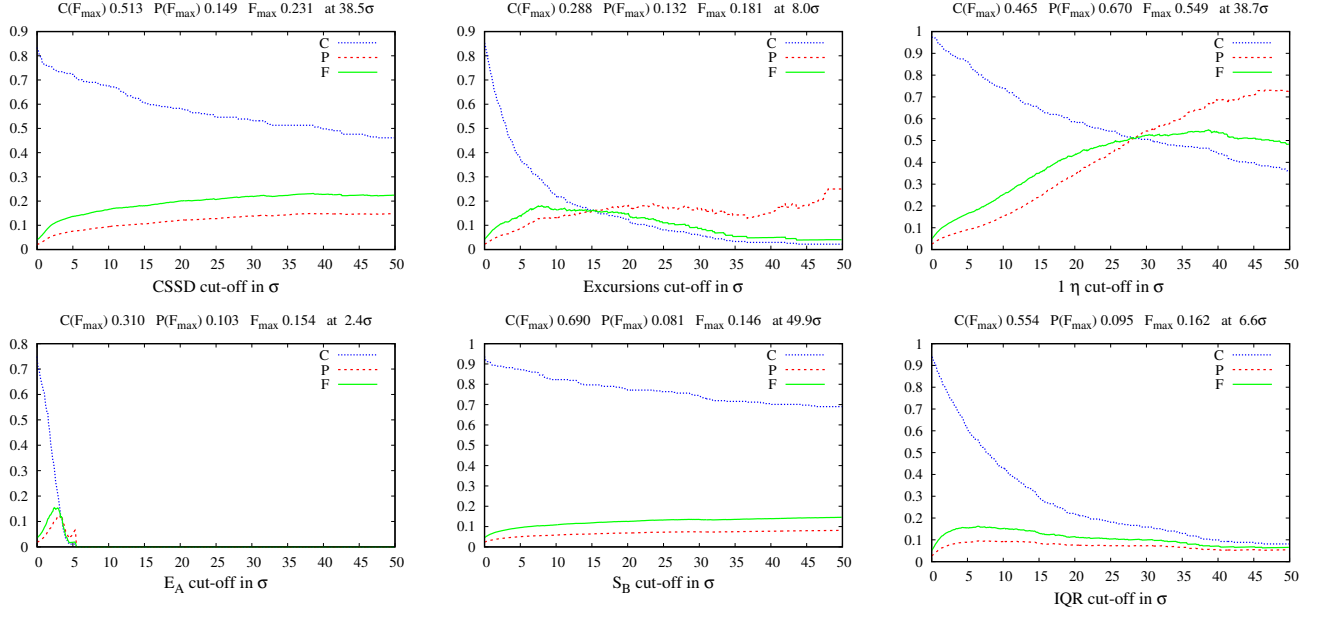
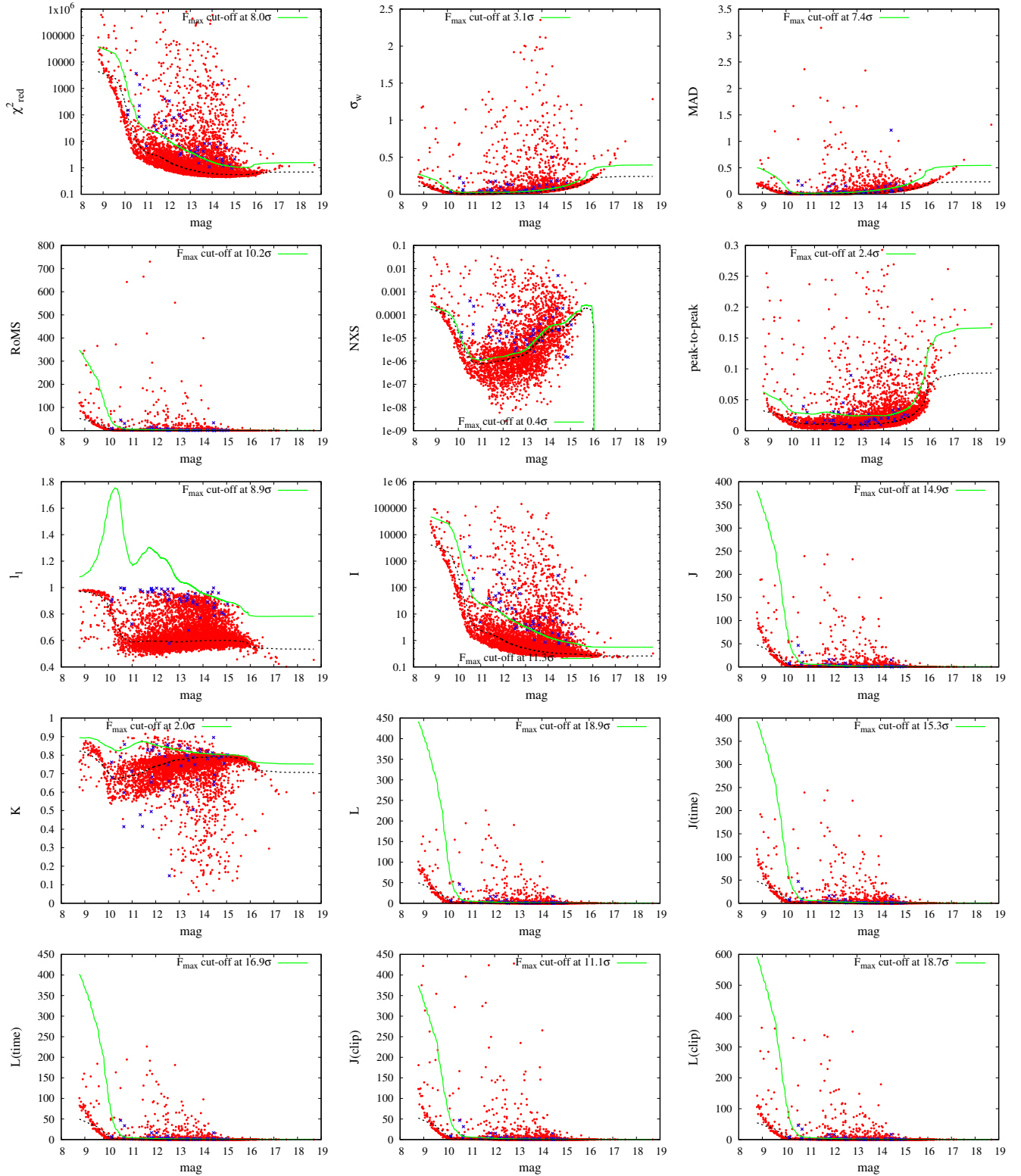


Figure 10, continued.



**Figure 11.** Variability indices defined in Sec. 2 as functions of magnitude for the TF2 dataset described in Sec. 3.1. Variable objects are marked with 'x'. The curves represent the expected value of an index as a function of magnitude and the selection threshold corresponding to the best trade-off between the completeness and purity of the candidates list ( $F_{\text{max}}$ , see Sec. 4, Fig. 12).

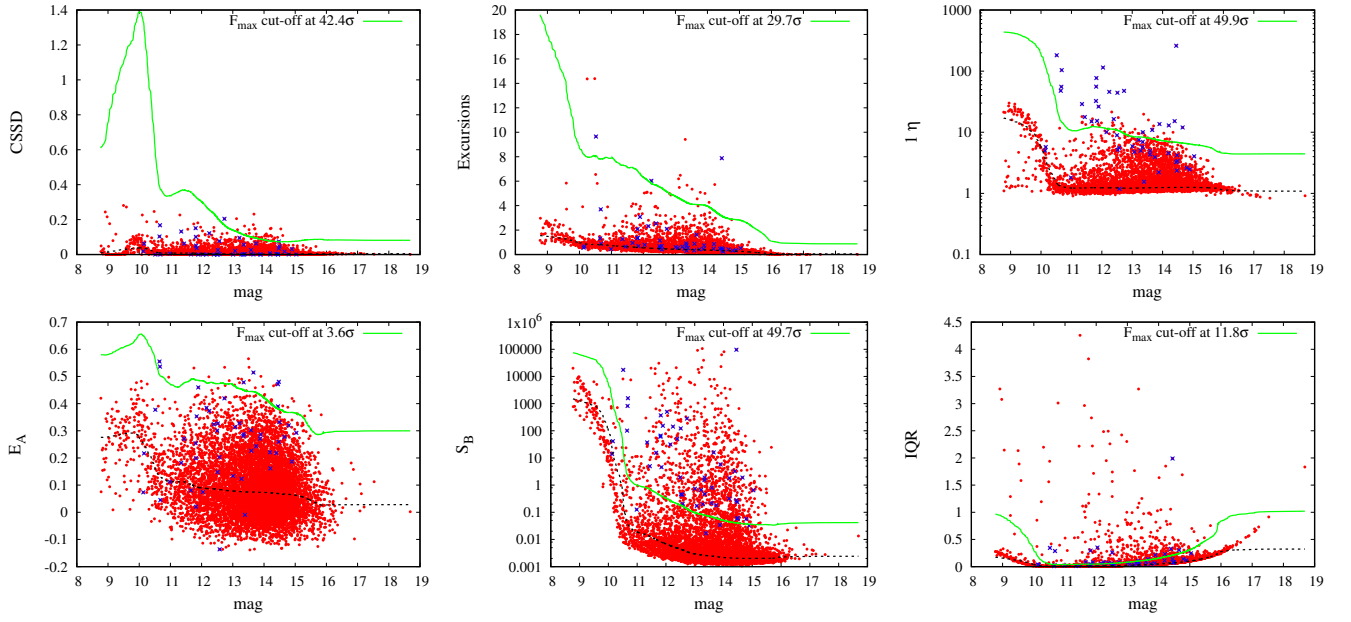
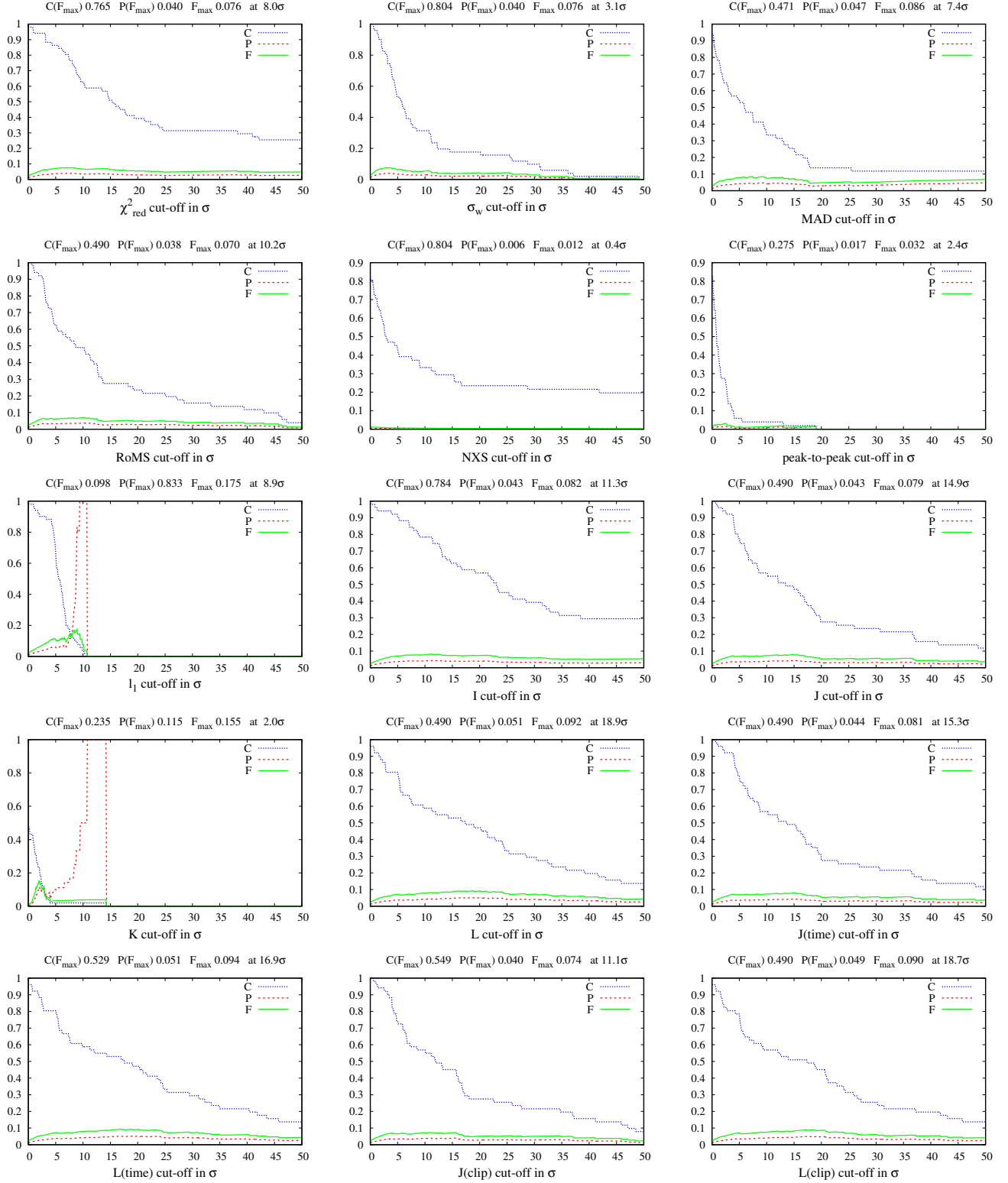


Figure 11. continued.



**Figure 12.** Variable star selection completeness (C), purity (P), and  $F_1$ -score (F, see Sec 4) as a function of selection threshold for the variability indices defined in Sec. 2 (TF2 dataset, Sec. 3.1).

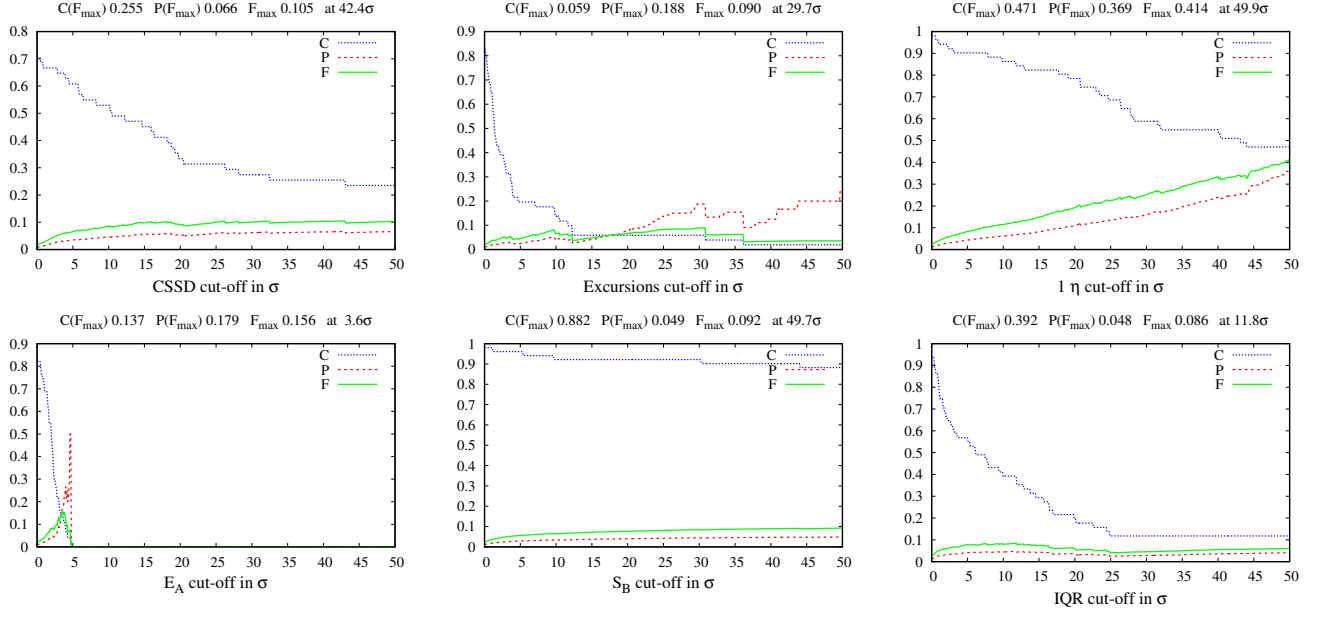
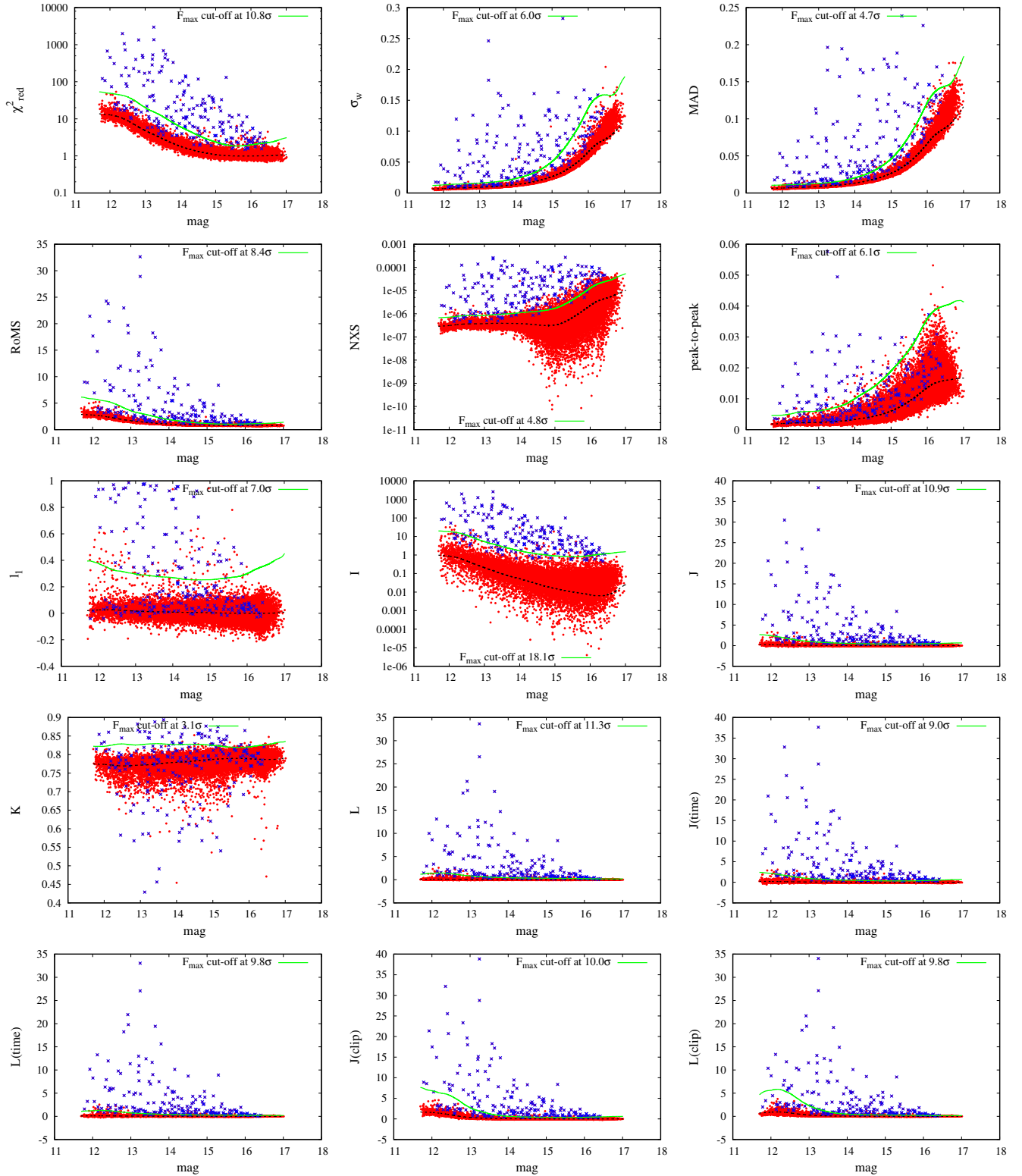


Figure 12. continued.



**Figure 13.** Variability indices defined in Sec. 2 as functions of magnitude for the Krasnoyarsk dataset described in Sec. 3.2. Variable objects are marked with 'x'. The curves represent the expected value of an index as a function of magnitude and the selection threshold corresponding to the best trade-off between the completeness and purity of the candidates list ( $F_{\max}$ , see Sec. 4, Fig. 14).

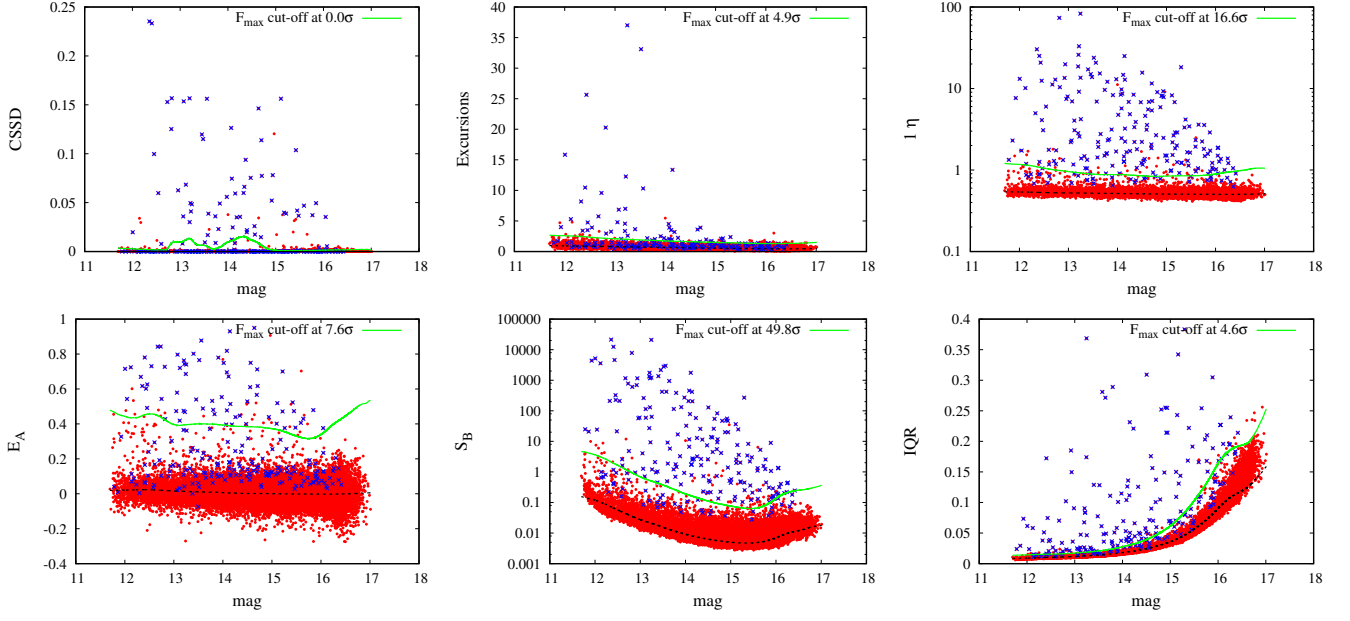
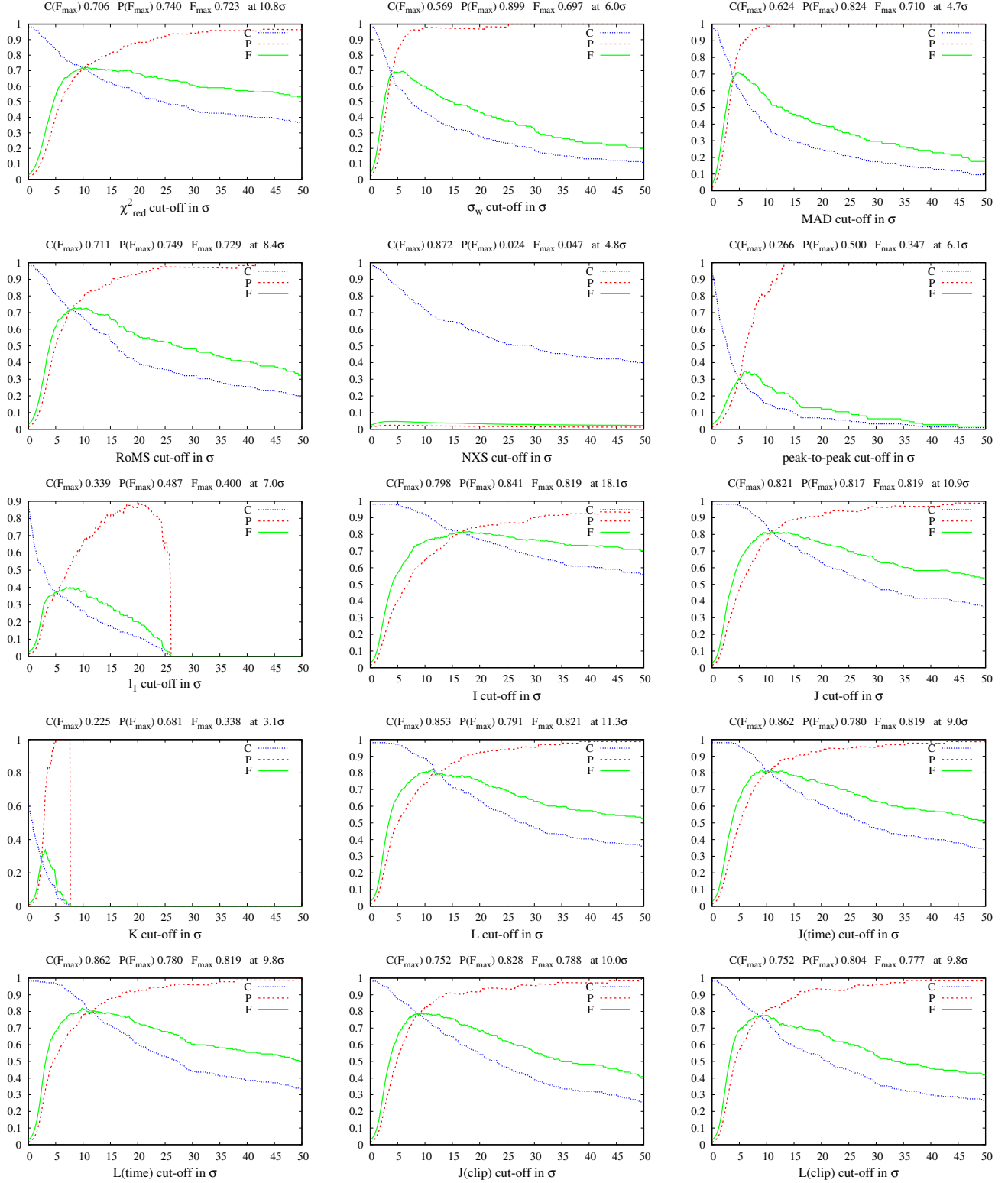


Figure 13. continued.





**Figure 14.** Variable star selection completeness (C), purity (P), and  $F_1$ -score (F, see Sec 4) as a function of selection threshold for the variability indices defined in Sec. 2 (Krasnoyarsk dataset, Sec. 3.2).

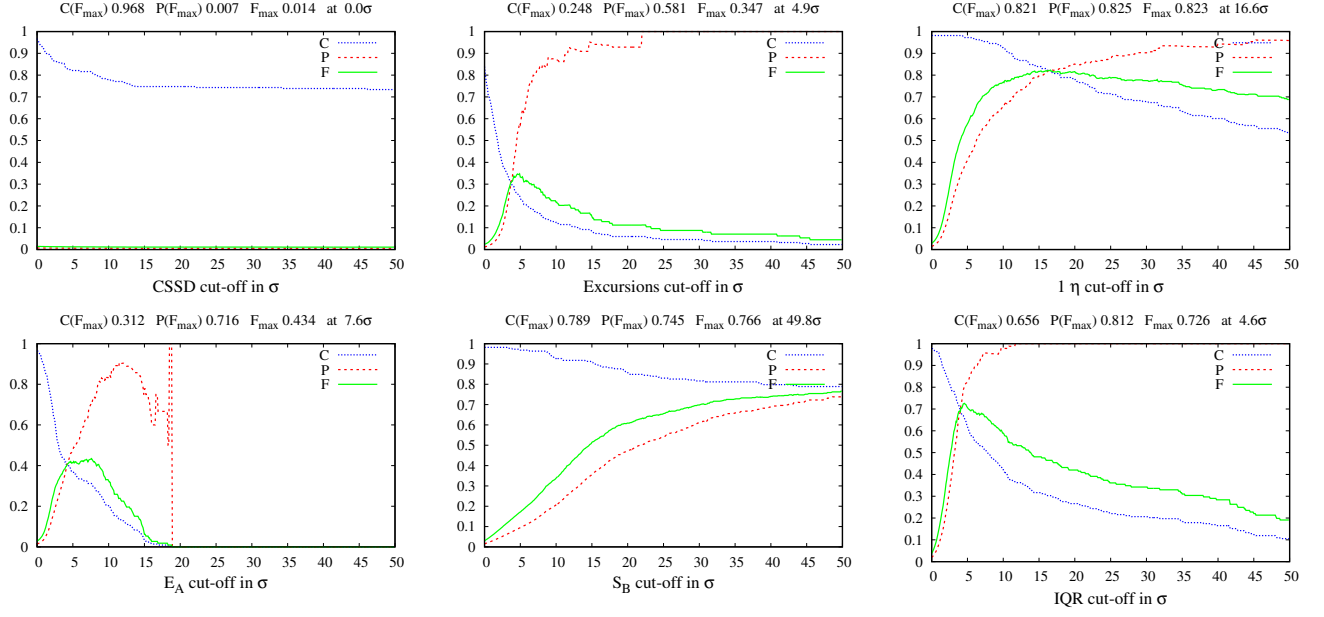
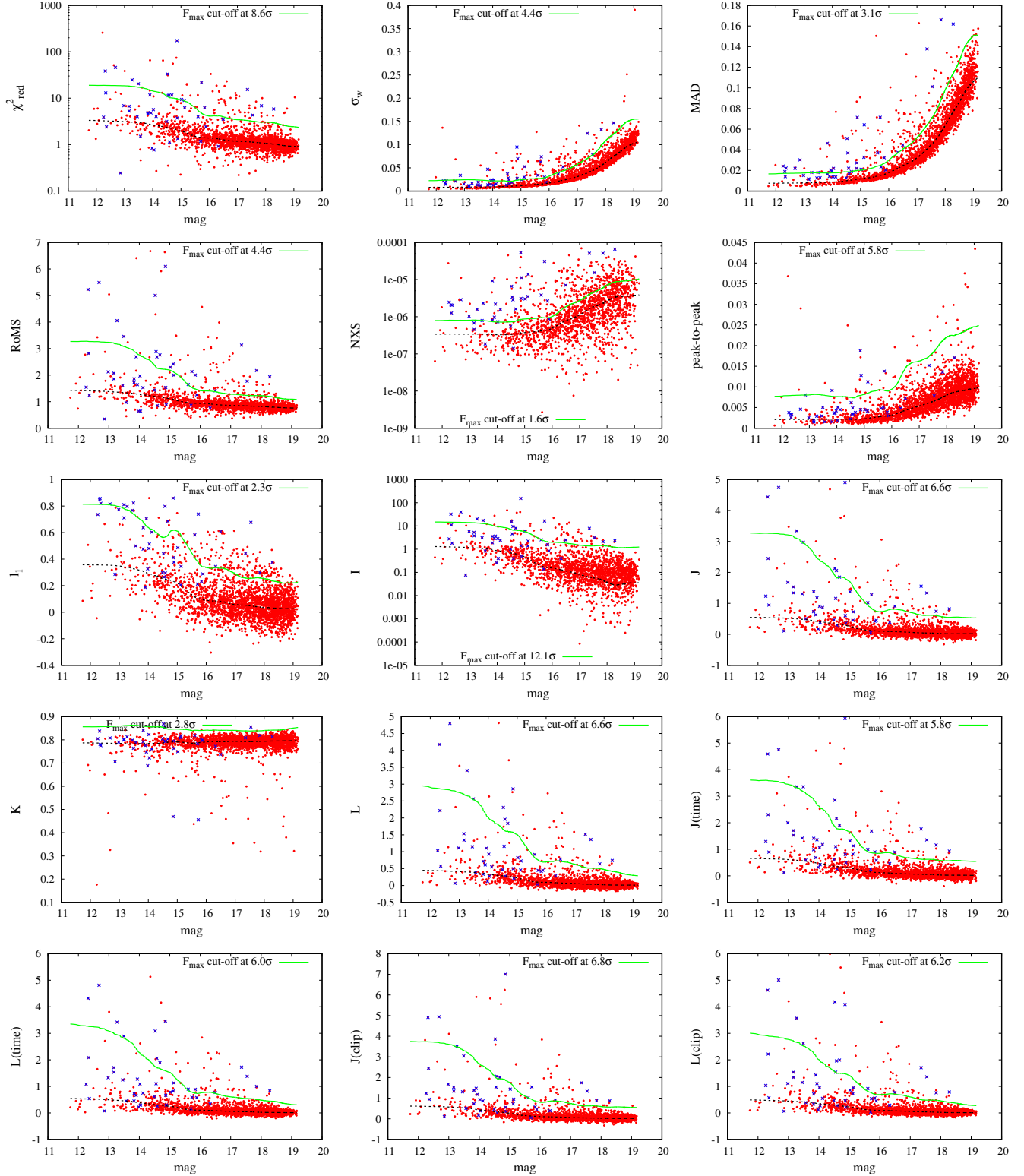


Figure 14. continued.



**Figure 15.** Variability indices defined in Sec. 2 as functions of magnitude for the Westerlund 1 dataset described in Sec. 3.3. Variable objects are marked with 'x'. The curves represent the expected value of an index as a function of magnitude and the selection threshold corresponding to the best trade-off between the completeness and purity of the candidates list ( $F_{\max}$ , see Sec. 4, Fig. 16).

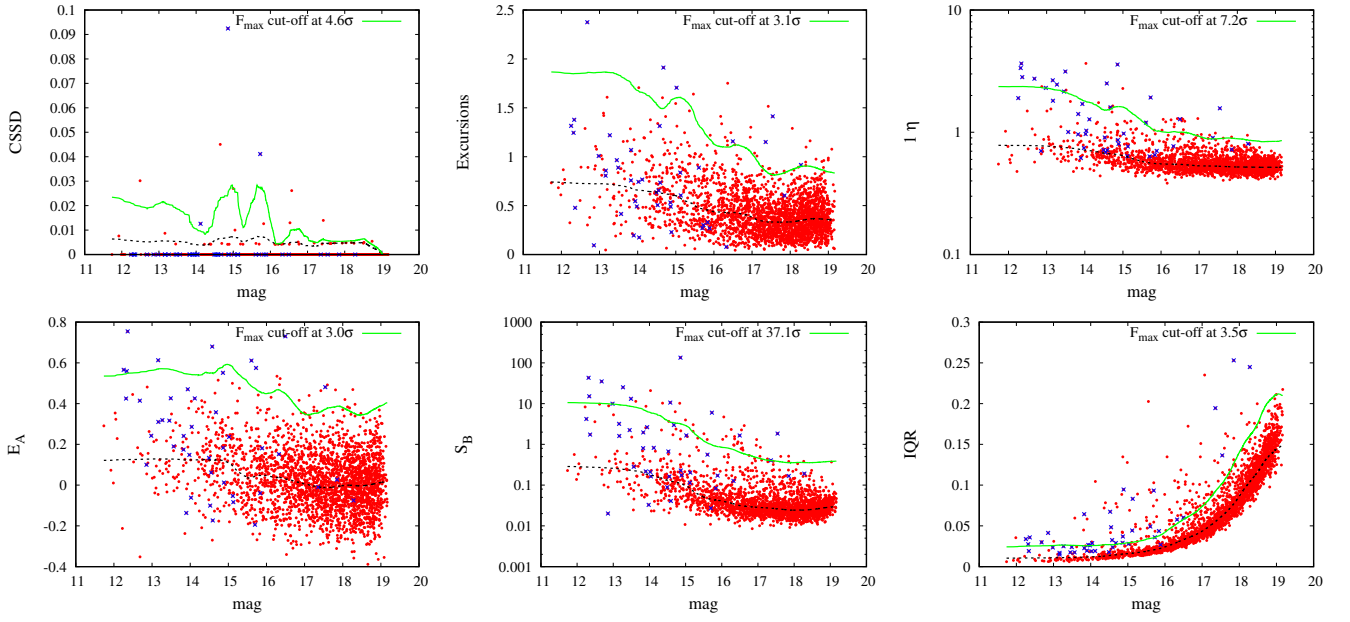
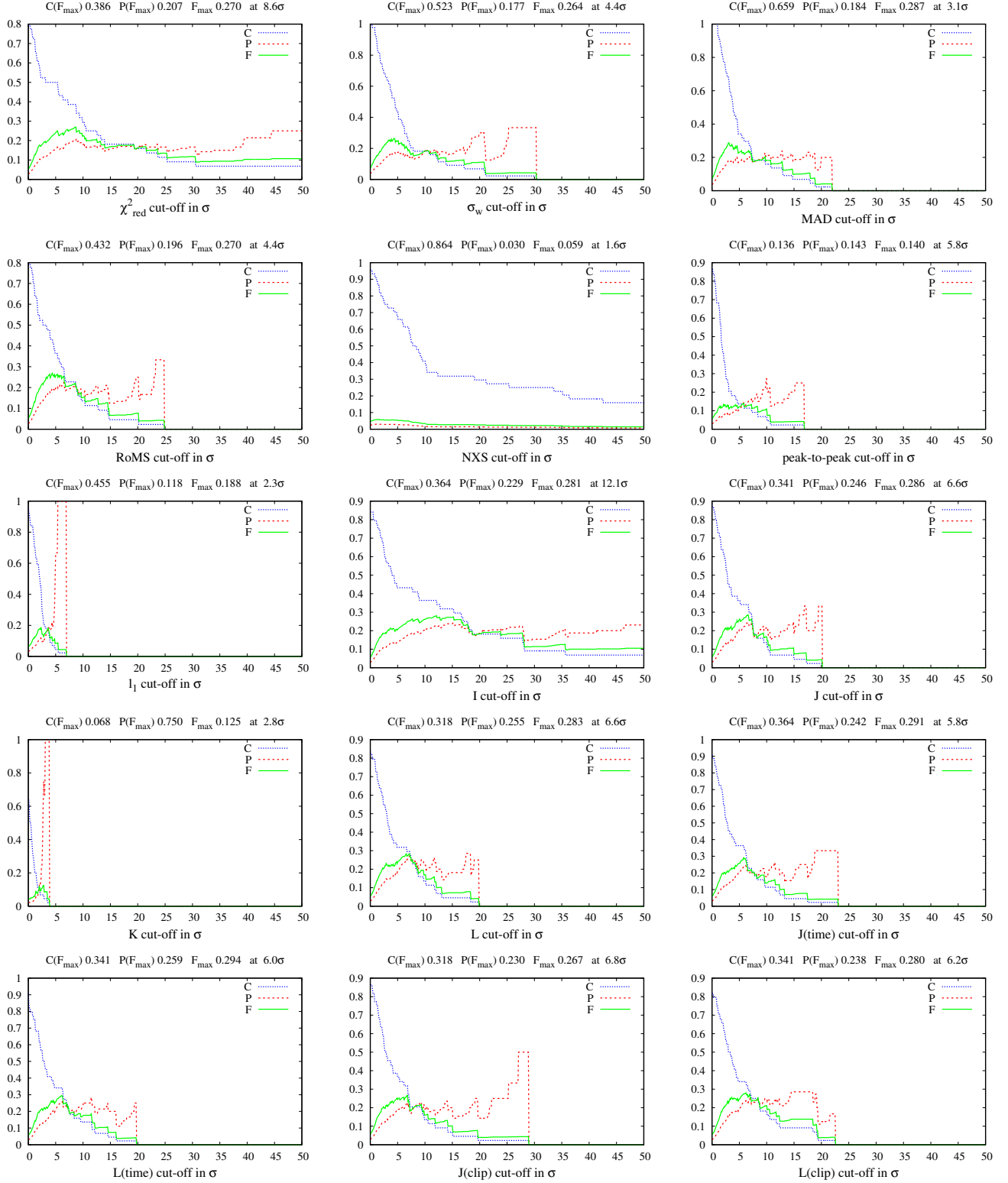


Figure 15. continued.



**Figure 16.** Variable star selection completeness (C), purity (P), and  $F_1$ -score (F, see Sec 4) as a function of selection threshold for the variability indices defined in Sec. 2 (Westerlund 1 dataset, Sec. 3.3).

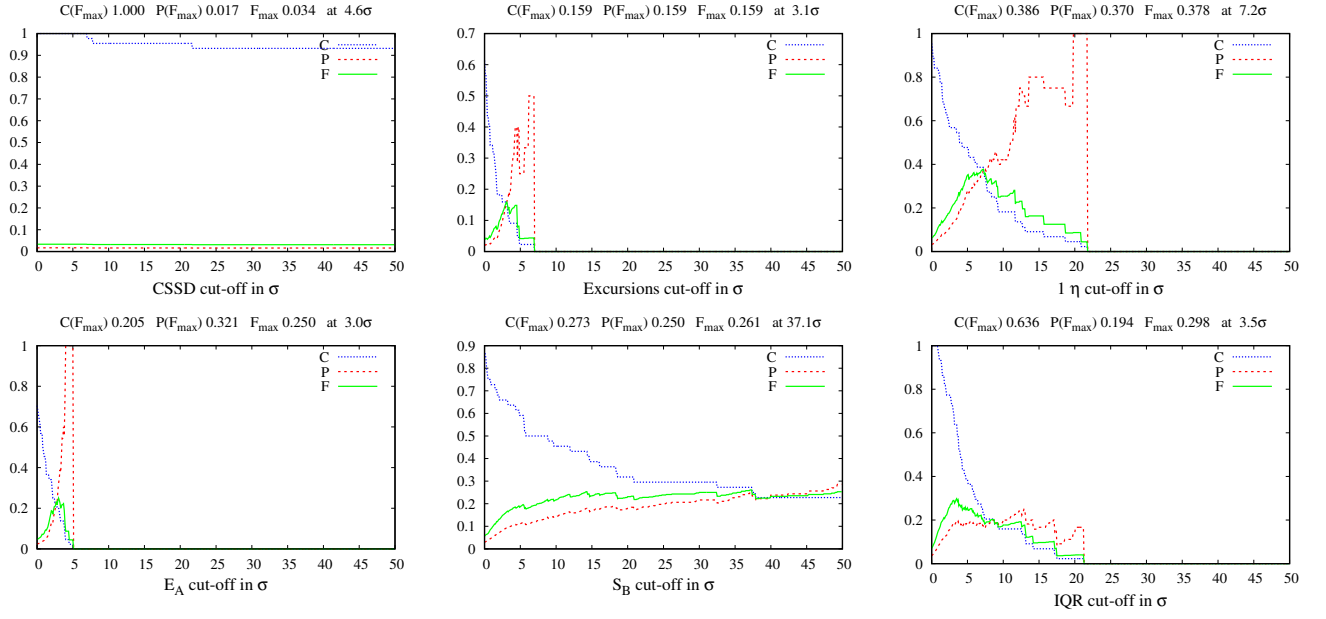
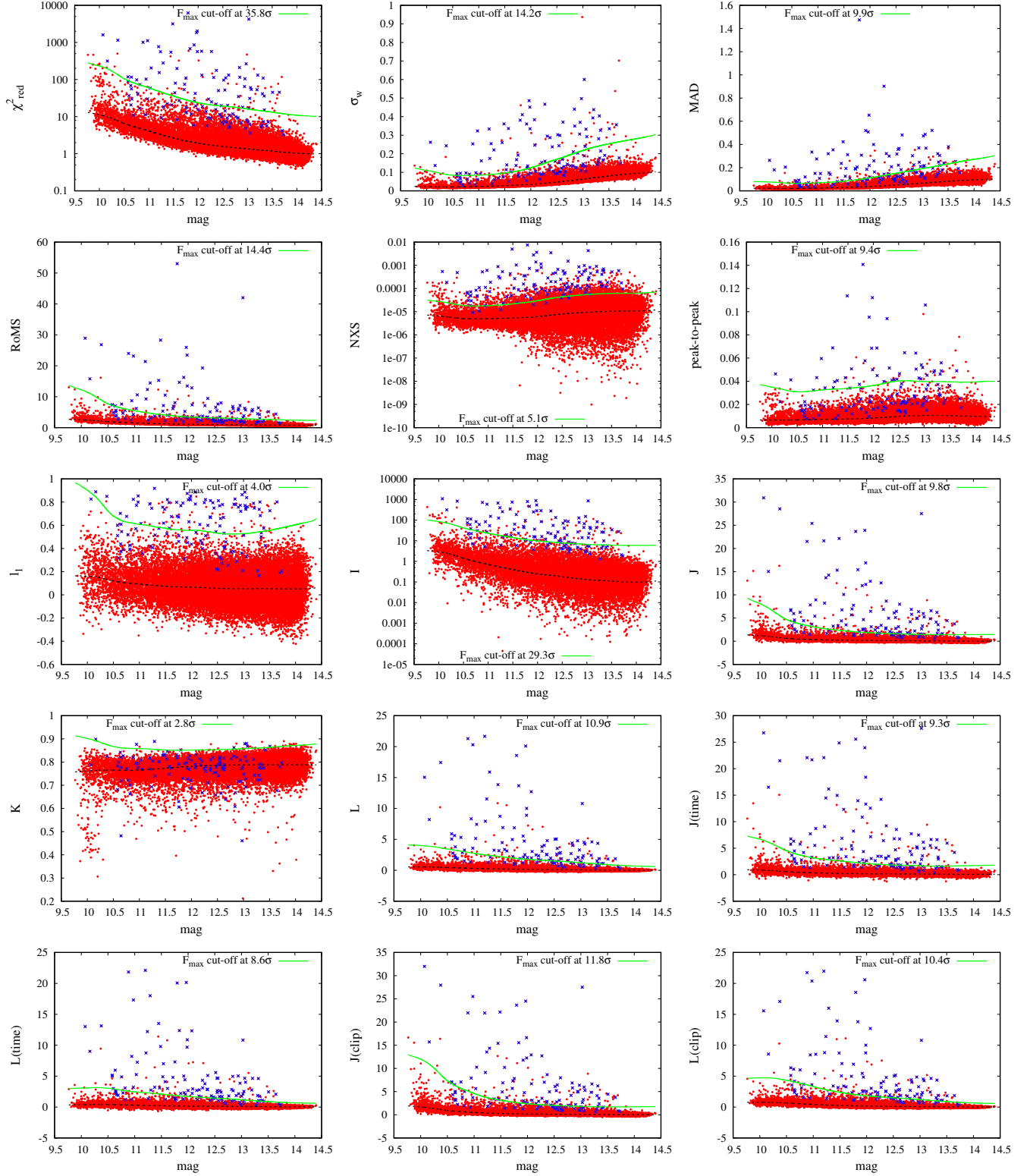


Figure 16. continued.



**Figure 17.** Variability indices defined in Sec. 2 as functions of magnitude for the And 1 dataset described in Sec. 3.4. Variable objects are marked with 'x'. The curves represent the expected value of an index as a function of magnitude and the selection threshold corresponding to the best trade-off between the completeness and purity of the candidates list ( $F_{\max}$ , see Sec. 4, Fig. 18).

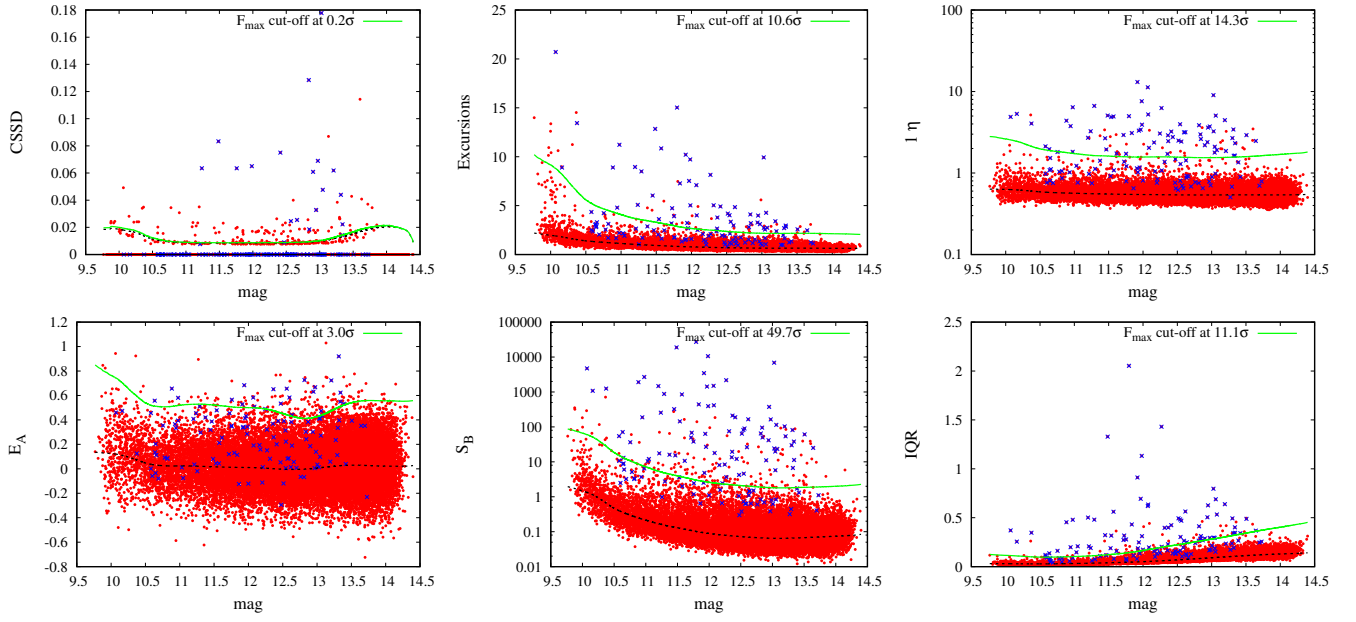
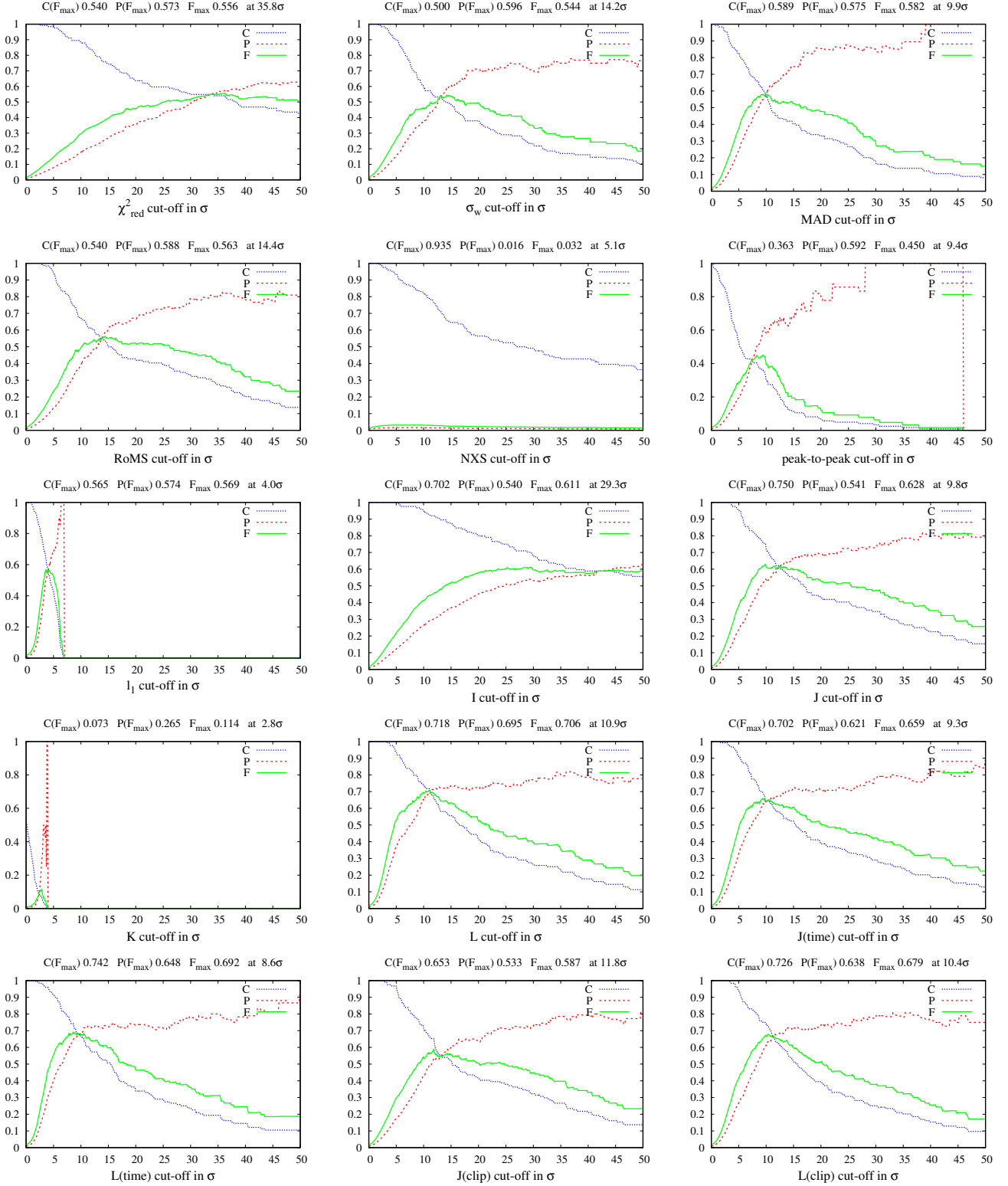


Figure 17. continued.





**Figure 18.** Variable star selection completeness (C), purity (P), and  $F_1$ -score (F, see Sec 4) as a function of selection threshold for the variability indices defined in Sec. 2 (And 1 dataset, Sec. 3.4).

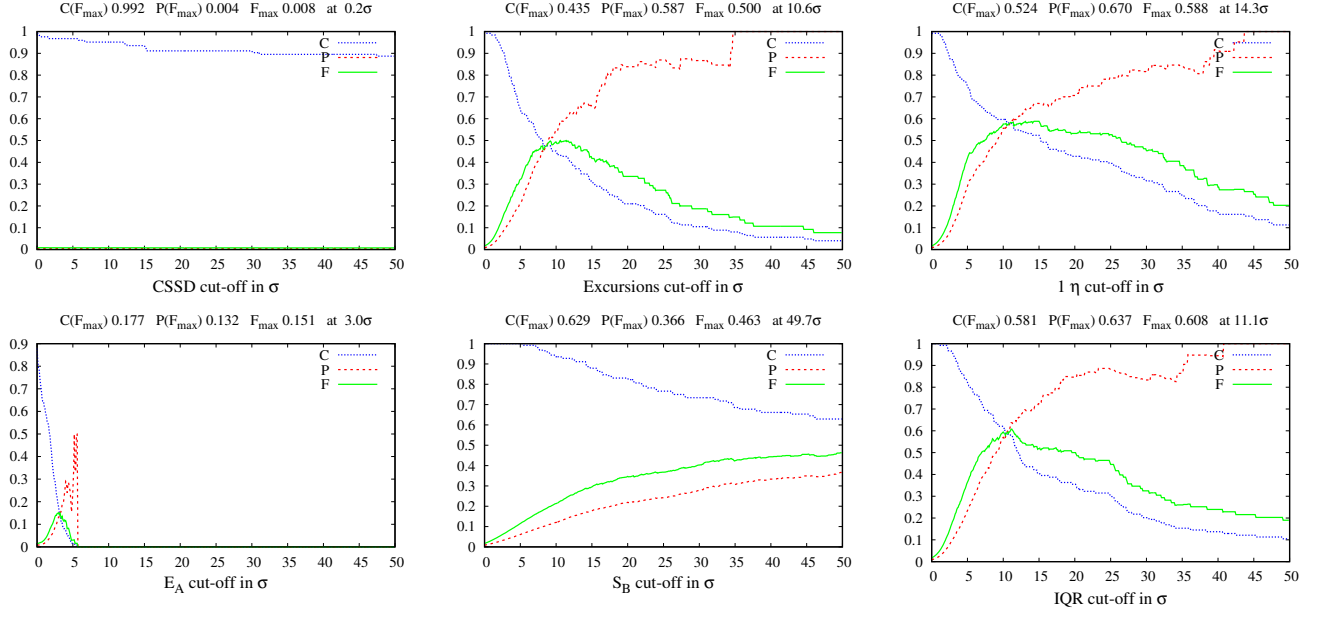
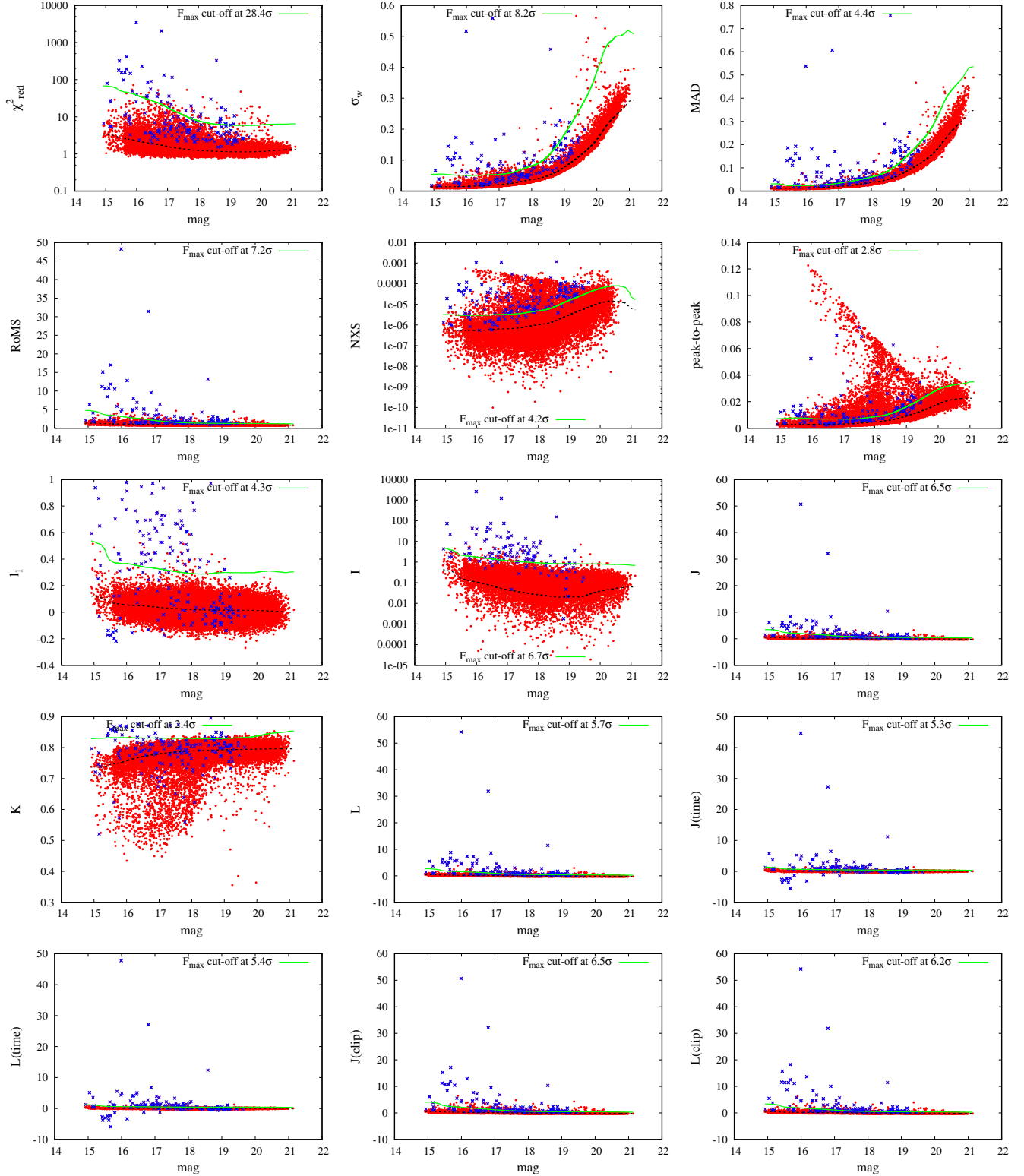


Figure 18. continued.



**Figure 19.** Variability indices defined in Sec. 2 as functions of magnitude for the OGLE-II LMC\_SC20 dataset described in Sec. 3.5. Variable objects are marked with 'x'. The curves represent the expected value of an index as a function of magnitude and the selection threshold corresponding to the best trade-off between the completeness and purity of the candidates list ( $F_{\text{max}}$ , see Sec. 4, Fig. 20).

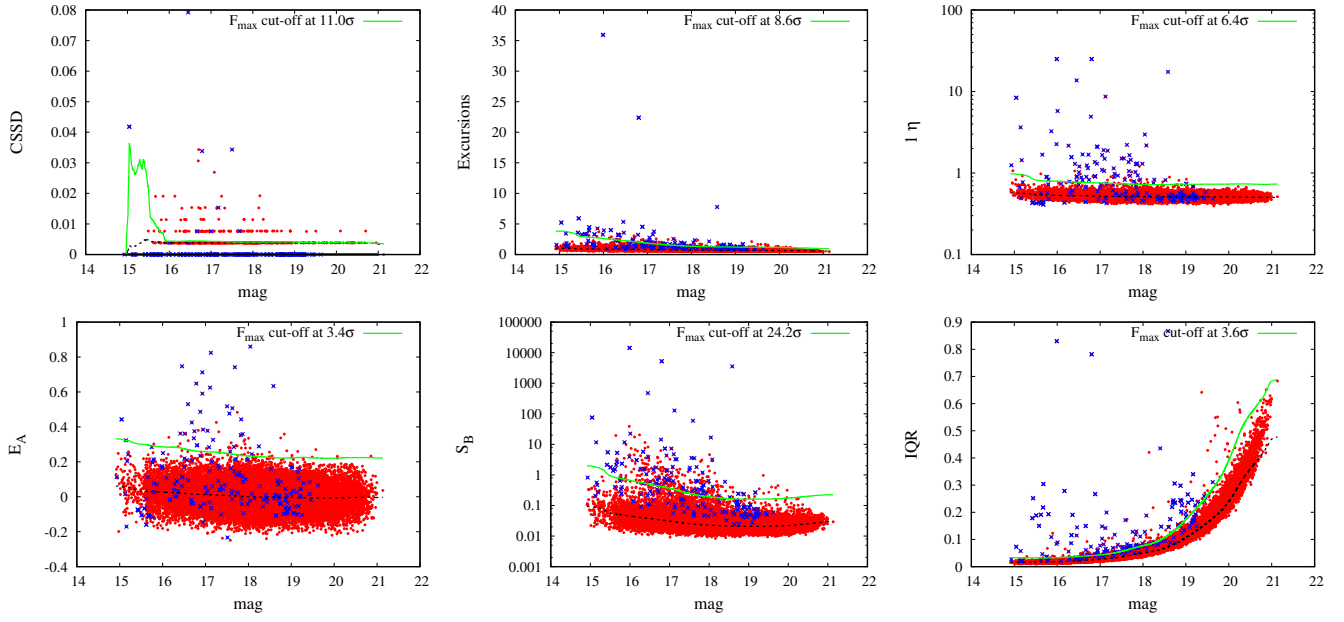
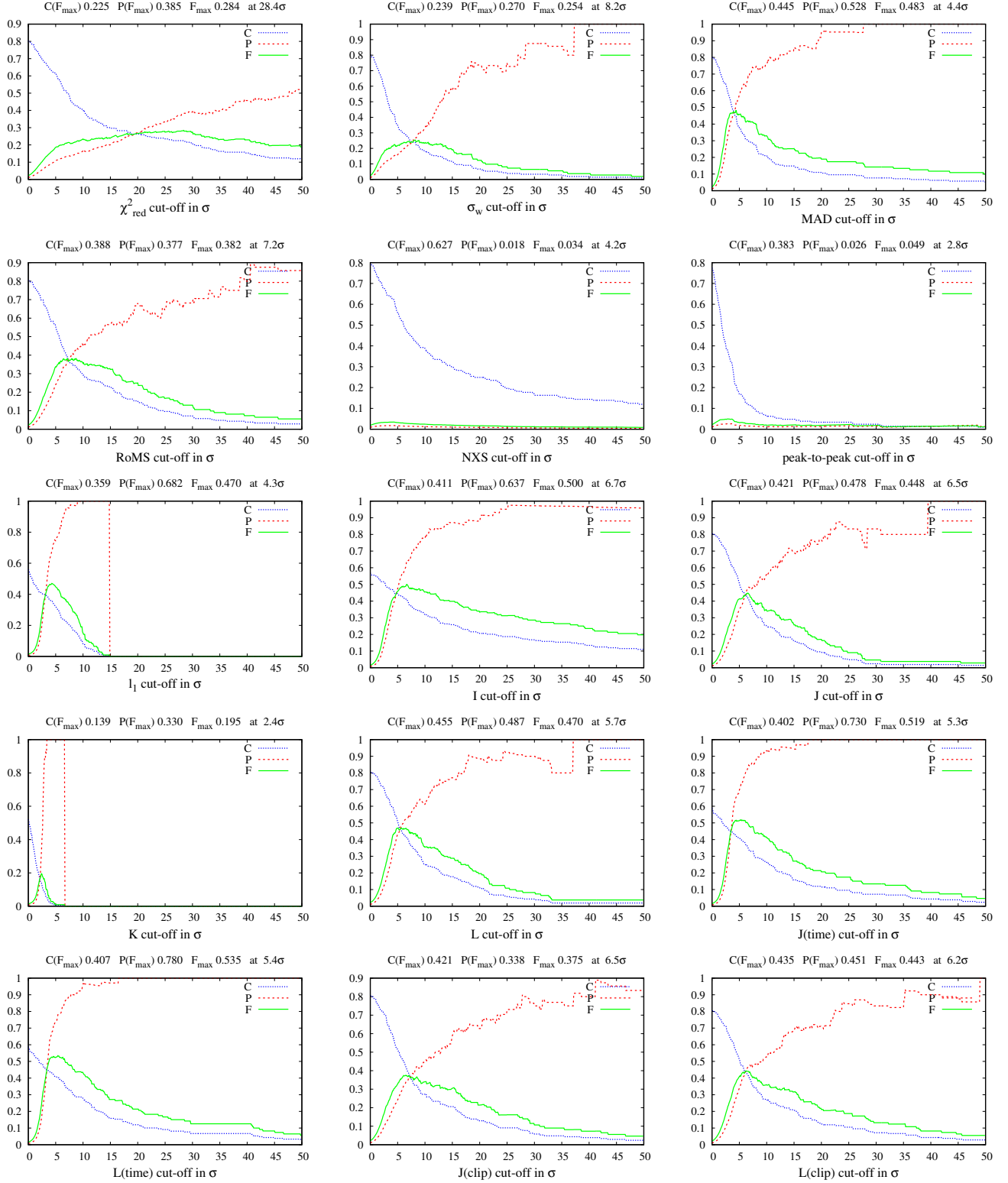


Figure 19. continued.



**Figure 20.** Variable star selection completeness (C), purity (P), and  $F_1$ -score (F, see Sec 4) as a function of selection threshold for the variability indices defined in Sec. 2 (OGLE-II LMC\_SC20 dataset, Sec. 3.5).

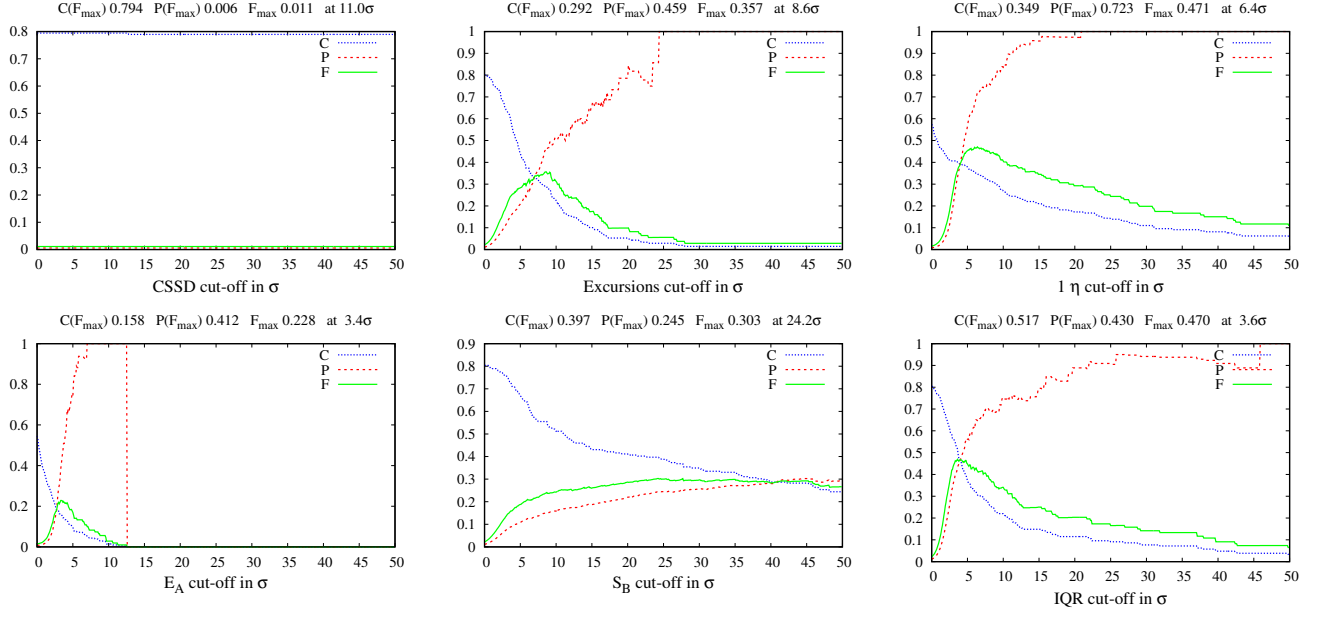
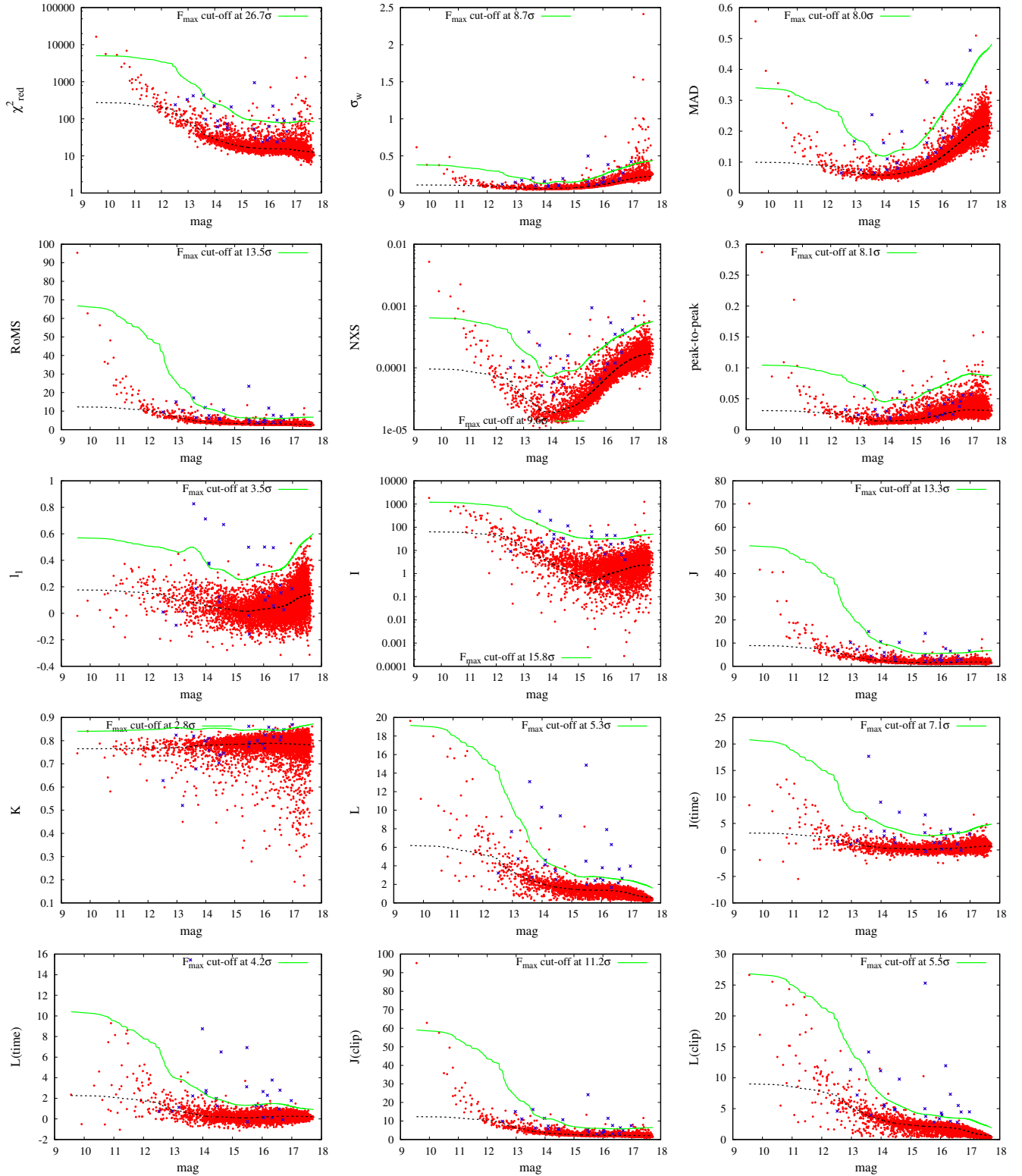


Figure 20. continued.



**Figure 21.** Variability indices defined in Sec. 2 as functions of magnitude for the 66 Oph dataset described in Sec. 3.6. Variable objects are marked with 'x'. The curves represent the expected value of an index as a function of magnitude and the selection threshold corresponding to the best trade-off between the completeness and purity of the candidates list ( $F_{\max}$ , see Sec. 4, Fig. 22).

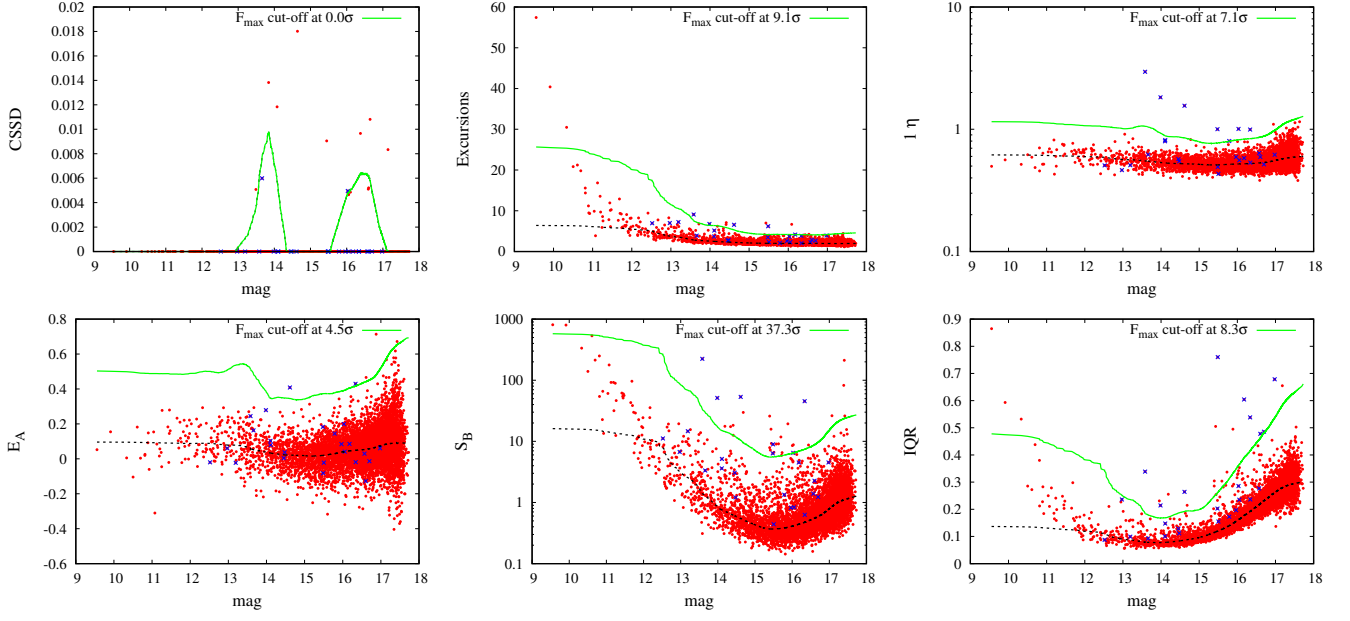


Figure 21. continued.





**Figure 22.** Variable star selection completeness (C), purity (P), and  $F_1$ -score (F, see Sec 4) as a function of selection threshold for the variability indices defined in Sec. 2 (66 Oph dataset, Sec. 3.6).

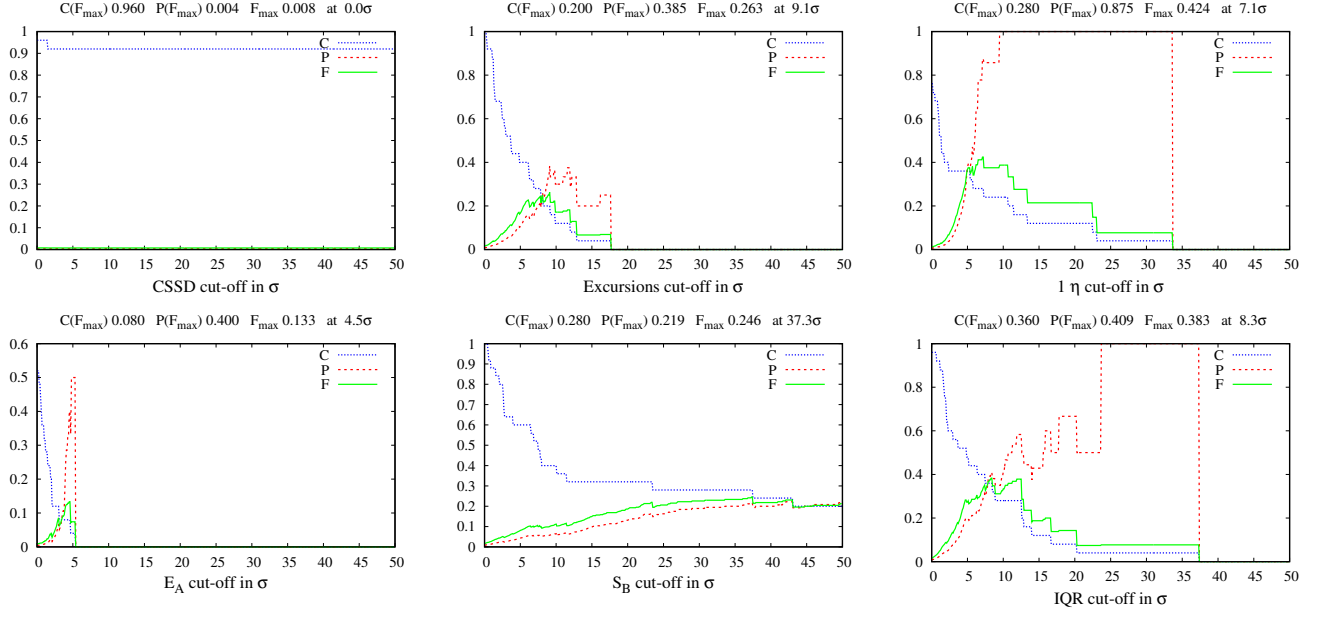
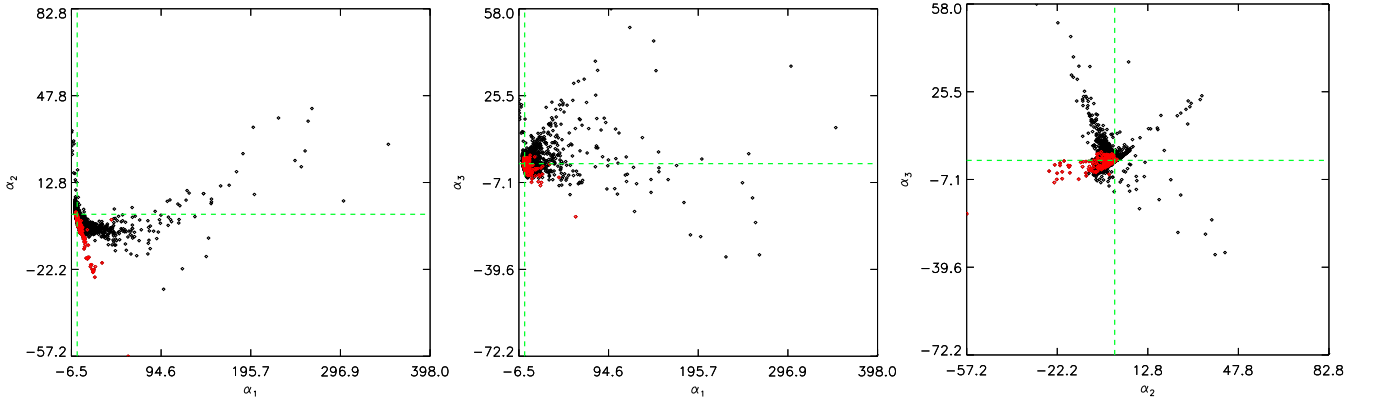
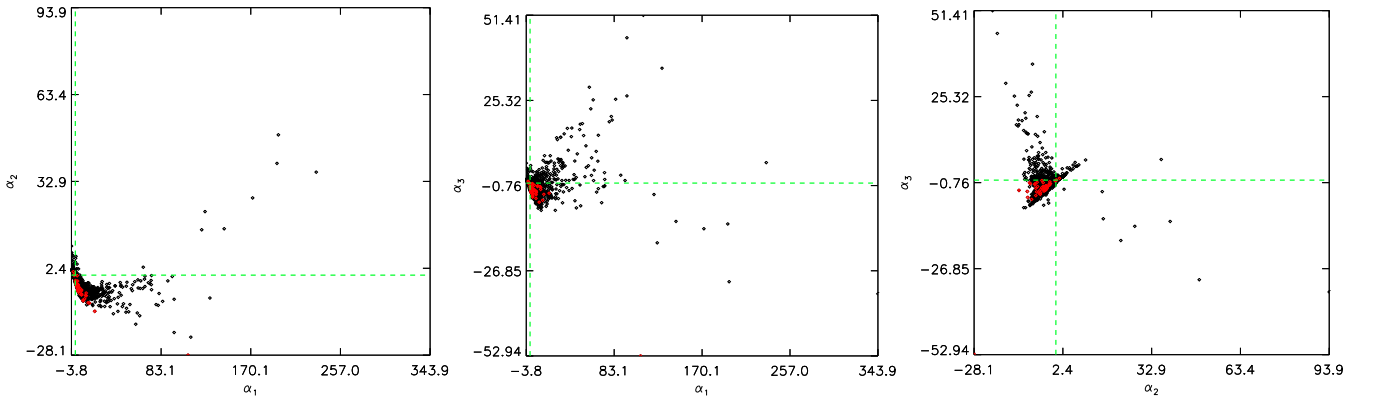
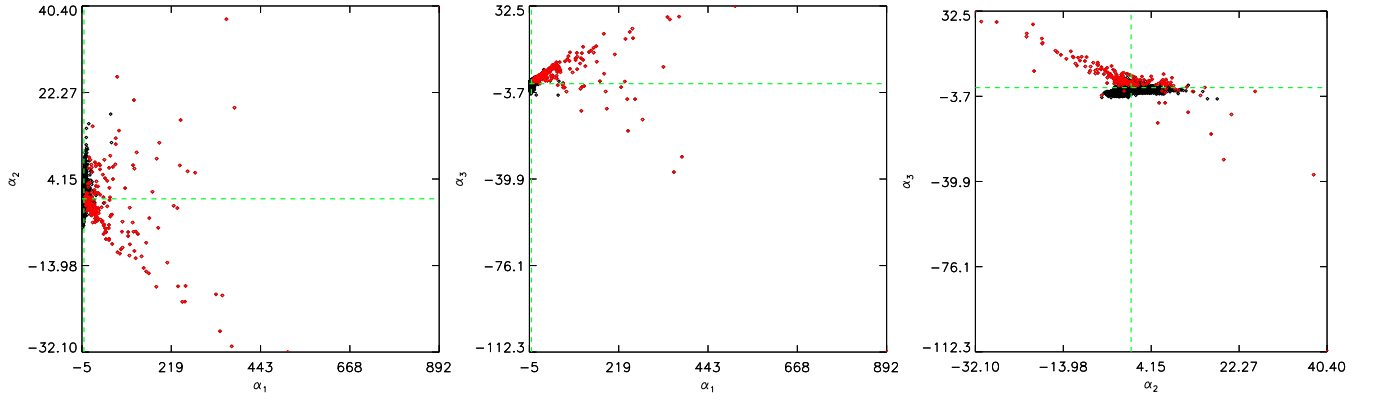
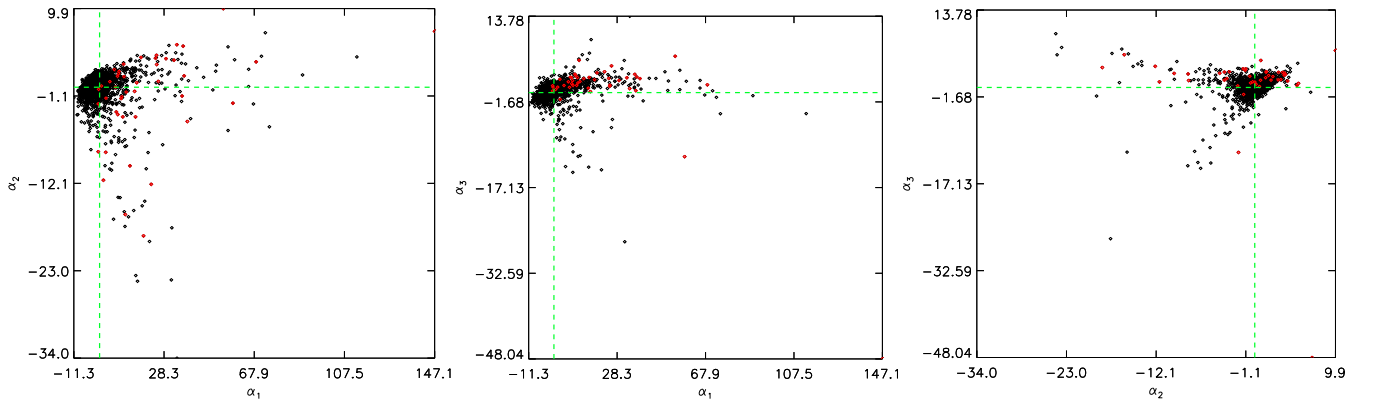


Figure 22. continued.

Figure 23. The admixture coefficients corresponding to PC1 ( $\alpha_1$ ), PC2 ( $\alpha_2$ ), and PC3 ( $\alpha_3$ ) for the TF1 dataset (Sec. 3.1). Variable stars are marked in red.Figure 24. The admixture coefficients corresponding to PC1 ( $\alpha_1$ ), PC2 ( $\alpha_2$ ), and PC3 ( $\alpha_3$ ) for the TF2 dataset (Sec. 3.1). Variable stars are marked in red.



**Figure 25.** The admixture coefficients corresponding to PC1 ( $\alpha_1$ ), PC2 ( $\alpha_2$ ), and PC3 ( $\alpha_3$ ) for the Kr dataset (Sec. 3.2). Variable stars are marked in red.



**Figure 26.** The admixture coefficients corresponding to PC1 ( $\alpha_1$ ), PC2 ( $\alpha_2$ ), and PC3 ( $\alpha_3$ ) for the W1 dataset (Sec. 3.3). Variable stars are marked in red.

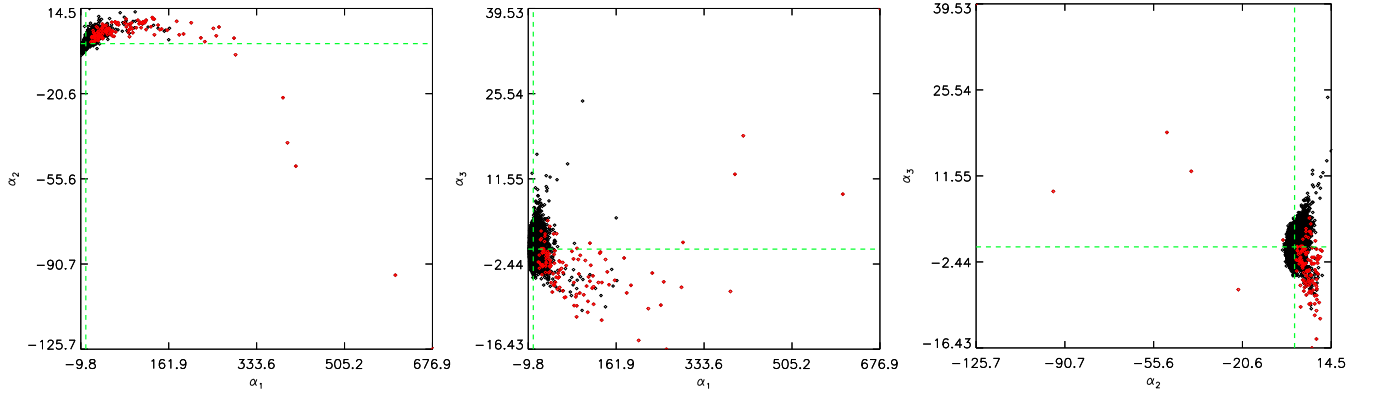


**Figure 27.** The admixture coefficients corresponding to PC1 ( $\alpha_1$ ), PC2 ( $\alpha_2$ ), and PC3 ( $\alpha_3$ ) for the And1 dataset (Sec. 3.4). Variable stars are marked in red.

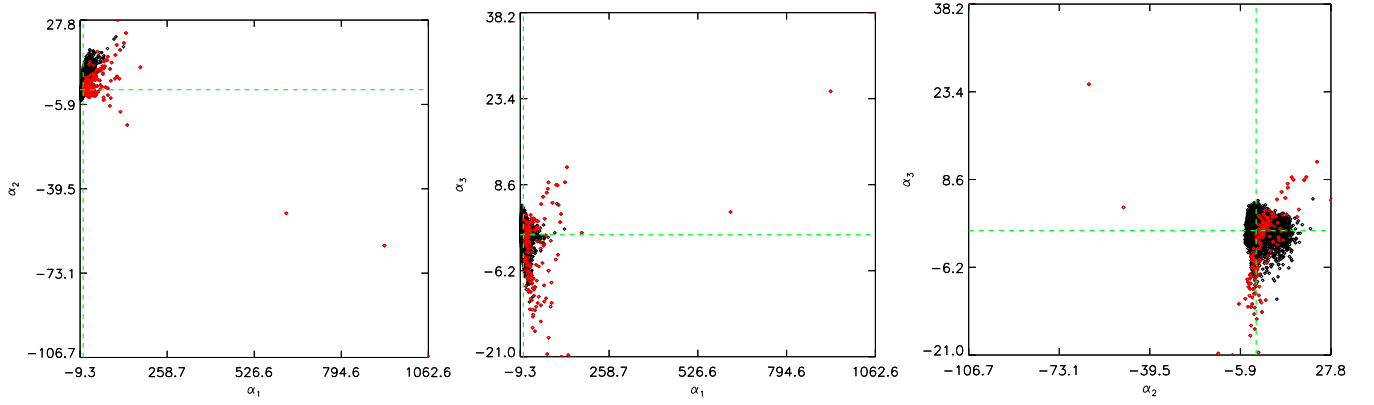


**Figure 28.** The admixture coefficients corresponding to PC1 ( $\alpha_1$ ), PC2 ( $\alpha_2$ ), and PC3 ( $\alpha_3$ ) for the OGLE dataset (Sec. 3.5). Variable stars are marked in red.

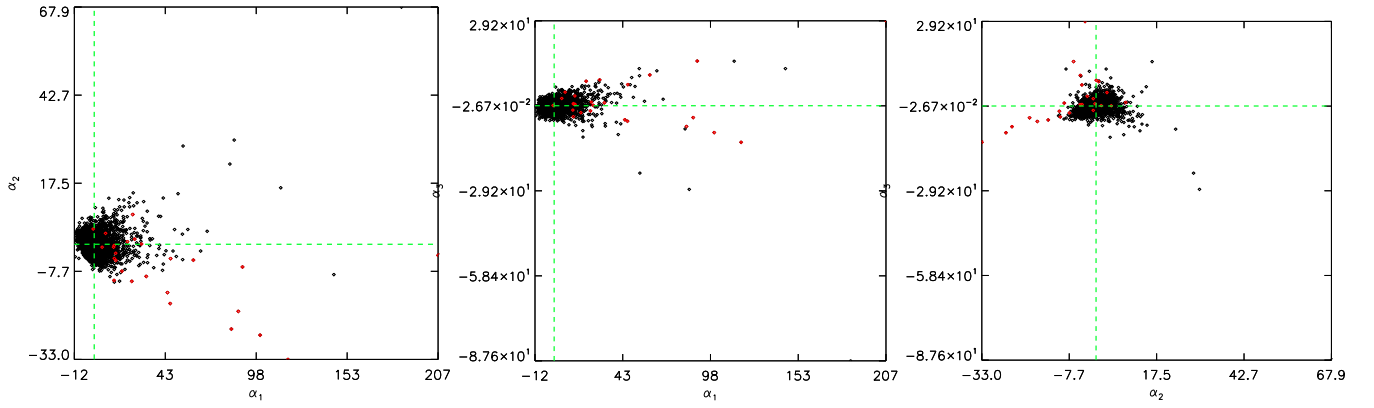


**Figure 29.** The admixture coefficients corresponding to PC1 ( $\alpha_1$ ), PC2 ( $\alpha_2$ ), and PC3 ( $\alpha_3$ ) for the 66Oph dataset (Sec. 3.6). Variable stars are marked in red.

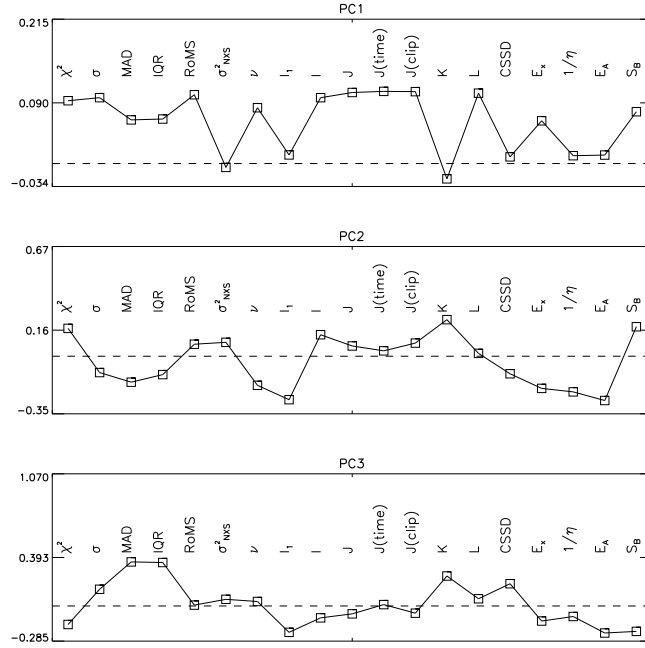


**Figure 30.** The first three principal components in the the TF1 dataset (Sec. 3.1). The dashed line indicates zero contribution of an index to the PC. Percentage of the total variance explained by PC1/PC2/PC3: 47.8/11.0/9.3.

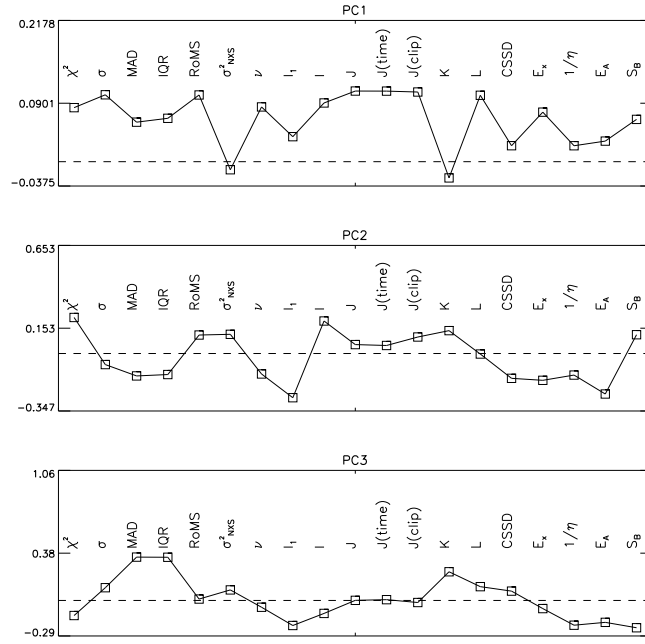


**Figure 31.** The first three principal components in the the TF2 dataset (Sec. 3.1). The dashed line indicates zero contribution of an index to the PC. Percentage of the total variance explained by PC1/PC2/PC3: 47.0/12.9/9.9.

This paper has been typeset from a  $\text{\LaTeX}$  file prepared by the author.

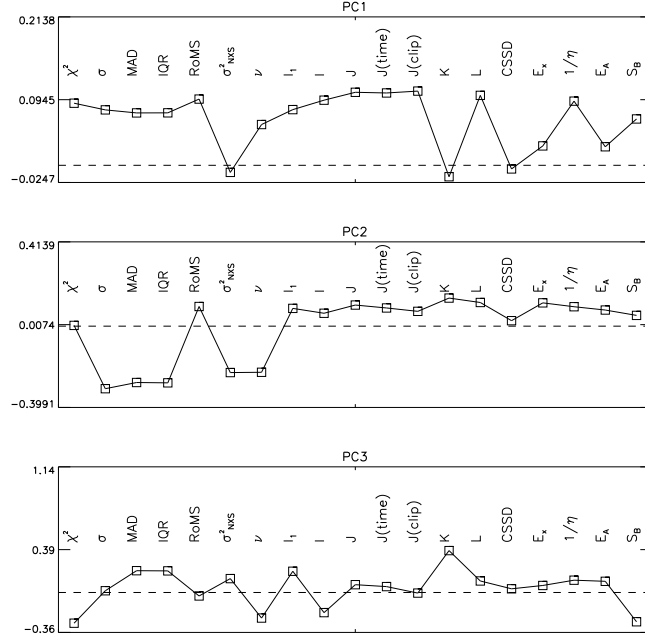


**Figure 32.** The first three principal components in the the W1 dataset (Sec. 3.3). The dashed line indicates zero contribution of an index to the PC. Percentage of the total variance explained by PC1/PC2/PC3: 47.0/11.4/9.4.

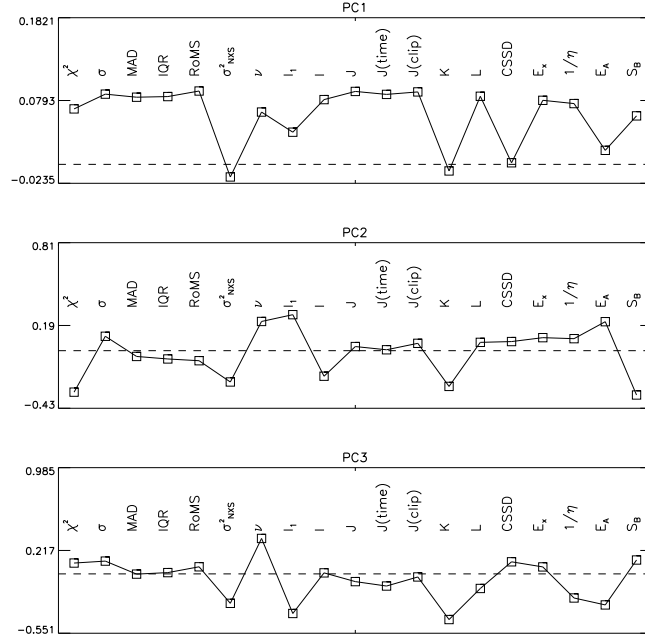


**Figure 33.** The first three principal components in the the And1 dataset (Sec. 3.4). The dashed line indicates zero contribution of an index to the PC. Percentage of the total variance explained by PC1/PC2/PC3: 55.9/8.8/7.2.

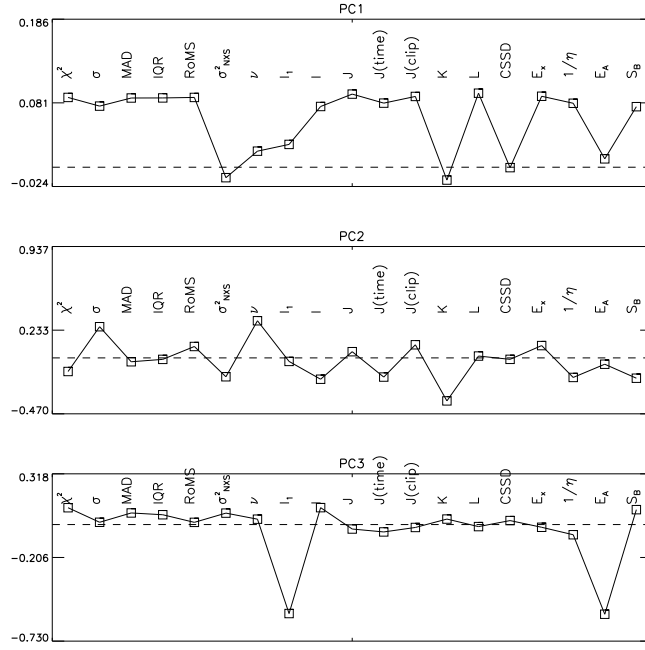


**Figure 34.** The first three principal components in the the OGLE dataset (Sec. 3.5). The dashed line indicates zero contribution of an index to the PC. Percentage of the total variance explained by PC1/PC2/PC3: 55.1/10.8/7.7.

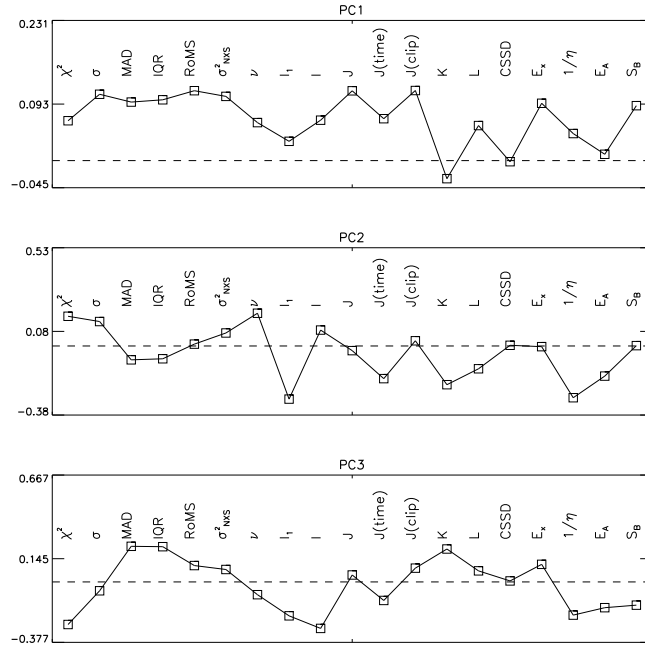


**Figure 35.** The first three principal components in the the 66Oph dataset (Sec. 3.6). The dashed line indicates zero contribution of an index to the PC. Percentage of the total variance explained by PC1/PC2/PC3: 42.3/13.9/10.6.

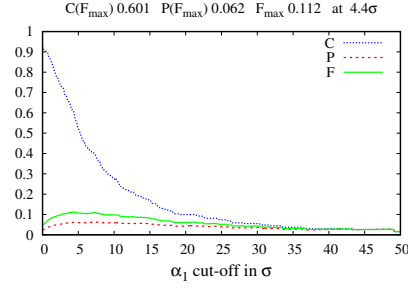


**Figure 36.** Variable star selection completeness (C), purity (P), and  $F_1$ -score (F; see Sec. 4) as a function of selection threshold for the admixture coefficient  $\alpha_1$  used as a composite variability index (Sec. 5.4) computed for the TF1 dataset (Sec. 3.1).

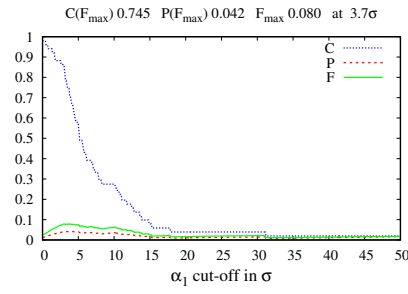


**Figure 37.** Variable star selection completeness (C), purity (P), and  $F_1$ -score (F; see Sec. 4) as a function of selection threshold for the admixture coefficient  $\alpha_1$  used as a composite variability index (Sec. 5.4) computed for the TF2 dataset (Sec. 3.1).

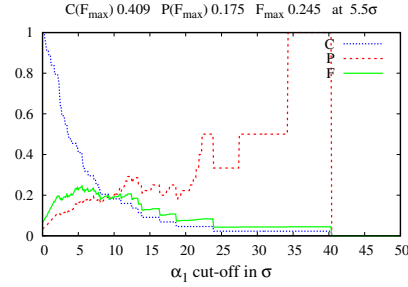


**Figure 38.** Variable star selection completeness (C), purity (P), and  $F_1$ -score (F; see Sec. 4) as a function of selection threshold for the admixture coefficient  $\alpha_1$  used as a composite variability index (Sec. 5.4) computed for the W1 dataset (Sec. 3.3).

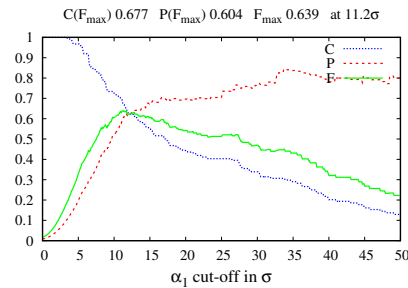


**Figure 39.** Variable star selection completeness (C), purity (P), and  $F_1$ -score (F; see Sec. 4) as a function of selection threshold for the admixture coefficient  $\alpha_1$  used as a composite variability index (Sec. 5.4) computed for the And1 dataset (Sec. 3.4).



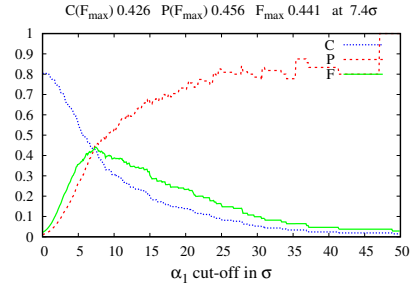


**Figure 40.** Variable star selection completeness (C), purity (P), and  $F_1$ -score (F; see Sec. 4) as a function of selection threshold for the admixture coefficient  $\alpha_1$  used as a composite variability index (Sec. 5.4) computed for the OGLE dataset (Sec. 3.5).

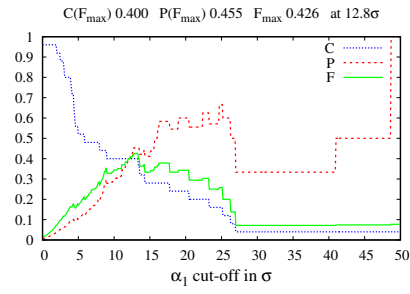


**Figure 41.** Variable star selection completeness (C), purity (P), and  $F_1$ -score (F; see Sec. 4) as a function of selection threshold for the admixture coefficient  $\alpha_1$  used as a composite variability index (Sec. 5.4) computed for the 66Oph dataset (Sec. 3.6).